Norwegian University of Science and Technology

Master's degree thesis

IP501909 MSc thesis, discipline oriented master

The Effect of Sloshing on a Tank Pressure Build-up Unit

10006 / Håvard Bolstad Banne

Number of pages including this page: 68

Aalesund, 06.06.17

Mandatory statement

Each student is responsible for complying with rules and regulations that relate to examinations and to academic work in general. The purpose of the mandatory statement is to make students aware of their responsibility and the consequences of cheating. **Failure to complete the statement does not excuse students from their responsibility.**

*Please complete the mandatory statement by placing a mark **in each box** for statements 1-6 below.*		
1.	**I/we herby declare that my/our paper/assignment is my/our own work, and that I/we have not used other sources or received other help than is mentioned in the paper/assignment.**	☒
2.	**I/we herby declare that this paper** 1. Has not been used in any other exam at another department/university/university college 2. Is not referring to the work of others without acknowledgement 3. Is not referring to my/our previous work without acknowledgement 4. Has acknowledged all sources of literature in the text and in the list of references 5. Is not a copy, duplicate or transcript of other work	Mark each box: 1. ☒ 2. ☒ 3. ☒ 4. ☒ 5. ☒
3.	**I am/we are aware that any breach of the above will be considered as cheating, and may result in annulment of the examination and exclusion from all universities and university colleges in Norway for up to one year, according to the Act relating to Norwegian Universities and University Colleges, section 4-7 and 4-8 and Examination regulations .**	☒
4.	**I am/we are aware that all papers/assignments may be checked for plagiarism by a software assisted plagiarism check**	☒
5.	**I am/we are aware that NTNU will handle all cases of suspected cheating according to prevailing guidelines.**	☒
6.	**I/we are aware of the NTNU's rules and regulation for using**	

	sources.	☒

Publication agreement

ECTS credits: 30

Supervisor: Prof. Vilmar *Æsøy*

Agreement on electronic publication of master thesis

Author(s) have copyright to the thesis, including the exclusive right to publish the document (The Copyright Act §2).
All theses fulfilling the requirements will be registered and published in Brage, with the approval of the author(s).
Theses with a confidentiality agreement will not be published.

I/we hereby give NTNU the right to, free of charge, make the thesis available for electronic publication: ☒**yes** ☐**no**

Is there an agreement of confidentiality? ☐**yes** ☒**no**
(A supplementary confidentiality agreement must be filled in and included in this document)
- If yes: **Can the thesis be online published when the period of confidentiality is expired?** ☐**yes** ☐**no**

This master's thesis has been completed and approved as part of a master's degree programme at NTNU Ålesund. The thesis is the student's own independent work according to section 6 of Regulations concerning requirements for master's degrees of December 1st, 2005.

Date: 06.06.17

NTNU

Norwegian University of
Science and Technology

The Effect of Sloshing on a Tank Pressure Build-up Unit

Håvard Bolstad Banne

June 2017

MASTER THESIS

Department of Ocean Operations and Civil Engineering

Norwegian University of Science and Technology

Supervisor 1: Professor Vilmar Æsøy

Supervisor 2: Erlend Grotle

Preface

This Master's thesis has been carried out as part of the study programme Product- and System Design at NTNU Aalesund. The study programme focuses on preparing the students for work mainly in the maritime cluster surrounding the university both in Aalesund as well as in the neighboring municipalities. Thus, the taught subjects and assigned tasks are mostly related to the surrounding industry, where many of the students are likely to work after studies.

The thesis work presented in this report was performed during the spring semester of 2017. Initially starting with the project as part of a summer internship, being employed by NTNU and supervised by prof. Vilmar Æsøy, the internship was all about building the experimental rig and testing it, making sure everything worked properly. Having gotten some insight into how it worked, it felt natural to continue the work in a more theoretical perspective in form of this Master's thesis.

The rig was built to be used for Erlend Grotle's research as part of his PhD, and the experiments carried out during the thesis work is hoped to aid this research. As such, the thesis work has partly been carried out at the university's laboratory, where the experimental rig was placed. The laboratory has served as a part time office and research station during the thesis work.

Ålesund, 2017-06-06

Håvard Bolstad Banne

Acknowledgment

First of all, I would like to thank my supervisors for their help through this project. Professor Vilmar Æsøy, who hired me for a summer internship in 2016, which has culminated in this thesis, and Erlend Grotle, who has been of tremendous help throughout the semester. André Tranvåg, the laboratory supervisor at the university is also deserving of my gratitude for providing tools required to repair or modify the experimental rig when needed.

Secondly, I want to thank my parents, Ellinor and Karsten Banne, for being supportive during my years of study, and for being very understanding during my work with this thesis.

Lastly, I want to thank my friends and classmates for their encouragement, help and cooperation during these years.

H.B.B.

Executive Summary

This thesis work has aimed to identify how sloshing will affect a liquefied natural gas (LNG) fuel tank. The physical nature of LNG means it needs to be kept cooled and pressurized in order to remain in a liquid state. By implementing a pressure build-up unit (PBU) it is possible to pressurize the tank vaporizing the tank's contents, for the vapour then to return to tank in a loop, building pressure in the process. A tank pressure build-up unit has been built in the laboratory at the university, which will be used for conducting experiments on sloshing.

To be able to perform calculations on the system, the efficiency of the electrical heater is found through a simple experiment, measuring the mass of water the heater is able to vaporize per minute, as well as measuring the electrical power used. Four different power settings are tested, showing that the relation between flow and power are close to linear, meaning that it is possible to interpolate the vaporized flow should one want to use a different power setting than the ones already tested. The electrical power tested ranges between 570-2019 W, with the efficiency ranging from 83.8-95.2%. The difference in efficiency is likely due to the water level rising when subject to higher levels of power, thus utilizing more of the heating coil, which is not fully submerged initially.

The heat loss of the system, or more specifically the heat transfer coefficient between the interior of the tank and its environment is found through logging of the system's temperature as the tank cools down, having initially been heated up to temperature of more than 110°C. Once the liquid and vapour temperature are equal, one can assume that no heat transfer is happening inside the tank, thus the following drop in temperature is due to heat loss to the surroundings. By recording the drop in temperature over a given time, the heat transfer coefficient is then calculated to be $U = 0.31 W/m^2 K$.

To find how sloshing affects this specific system, several tests are performed at different frequencies in order to observe how the severity of the sloshing affects the thermodynamical properties within the tank. The tank is heated to predetermined parameters, before the heater is turned off for the sloshing to be initiated, this in order to be in control over the amount of energy present in the system when the sloshing is performed. It is found that sloshing definitely increases heat and mass transfer over the liquid-vapour interface when compared to test conducted where no

tank motion is initiated. There is a clear distinction in heat and mass transfer between the different sloshing frequencies as well, where the general perception is that a higher frequency of sloshing results in a higher rate of energy transfer.

It is attempted to conduct a series of experiments where the heater is on during the tests, in order to see if compensation of the pressure drop during sloshing was possible. It is found that utilizing the heater does result in reduced drop in pressure, in addition to showing that pressure compensation is possible in lower frequencies with the electrical power at disposal for these experiments, albeit not entirely stable. With control regulation, compensation should work well.

The effect sloshing would have on heat and mass transfer was calculated from results gathered from the experiments. Calculating for a selection of tests with sloshing period ranging from T=2.50 seconds to T=4.00 seconds, as well as for a reference test with no tank excitation, it is found that sloshing at the lowest frequency tested, T=4.00 seconds, increases heat and mass transfer by 75% compared to the case with no tank excitation. The rate of heat and mass transfer increases as the sloshing frequency increases, calculations showing a 500% increase for sloshing period T=2.50 seconds.

List of Figures

List of Tables

Contents

Chapter 1

Introduction

1.1 Background and Motivation

Utilizing liquefied natural gas (LNG) as a fuel for ship transportation has shown great promise, due to its availability, cost effectiveness and environmental friendliness compared to traditional marine diesel oil (MDO). One of the issues of using LNG is the amount of space it requires in its gas state; hence, keeping it in a liquid state is a must. Implementing a pressure build-up unit (PBU) is one of several ways to design an LNG fuel system, due to the fact that it needs to be kept pressurized at low temperatures. The PBU keeps the tank pressurized, in addition to pushing the LNG through a vaporizer and into the engine, as shown in figure 1.1. Nonetheless, since it will require an enormous amount of energy to keep large quantities of LNG sufficiently cooled unpressurized, it will be easier, more practical and more economical to keep it pressurized.

Sloshing is generally a mostly unwanted behaviour of a liquid in a container, and has the potential to result in pressure drop within the tank, with engine shutdown as a possible consequence. The sloshing regime will thus be investigated, finding how the severity of the sloshing affect the system. This will likely be of great interest to the ship owners, which of course would like their solutions to be both economical and efficient.

As the tank will be subject to wave motion, it will be interesting to see how the system will react to the sloshing. Will the pressure and vapour temperature drop, and to which extent. The sloshing regime, or tank excited heat and mass transfer has been investigated for years, particularly in relation to fuel tanks in space rockets (Arndt (2011)), in addition to design of roads and

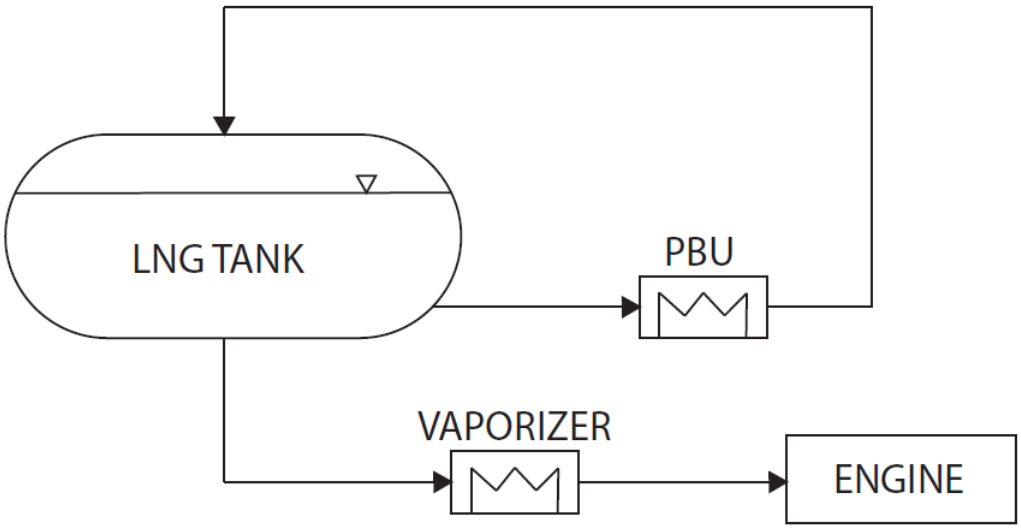

Figure 1.1: LNG system with PBU

dams, but the topic is still relatively new within the maritime sector in relation to LNG.

1.2 Literature Survey

It is shown by Ludwig et al. (2013) that periodic excitation of a liquid storage tank results in a pressure drop, and the dependency of the pressure drop on the wave amplitude is determined. Tests are performed on a partially filled cylindrical liquid nitrogen tank, with six different sloshing conditions performed. For the experiments, a pressure sensor and sixteen different silicon diodes designed for cryogenic conditions are installed at different levels of the tank. The sloshing motion in this case is radially linear, tank being mounted on a movable platform.

Three sloshing characteristics are identified during the experiments:

1. Stable planarwaves.
2. Chaotic sloshing: the wave amplitude is increasing until the downward wave crest acceleration is equal to the gravitational acceleration. Collapses rapidly before a new growth cycle begins.
3. Swirl wave: Very stable once established - grows to breaking conditions exponentially until stable.

Conclusive sloshing characteristics are hard to define, as the system is highly dynamic. Still, a certain categorization of the liquid motion may help understand what type of sloshing motion is the most severe. In relation to this thesis, the tank used is impossible to see inside of, making it necessary to properly analyze the results in order to find indications of the fluid motion.

From Das and Hopfinger (2009) it is shown that large amplitude wave motions increases condensation rate, compared to when the liquid-vapour interface is at rest, where pressure decrease due to condensation is small. Das and Hopfinger performs tests on a cylinder partially filled with liquid; the fluids used are low viscosity and low surface tension liquids of low boiling temperatures. Experiments are conducted with sub-cooled vapour filling the tank above the cold liquid. Attempting to produce mass transfer, the conditions of the experiments has been facilitated for condensation to take place. Contrary to the experiments that will be conducted in this thesis, Das and Hopfinger has control of the temperature of the testing cell, which in their case is heated to a temperature a few degrees below the saturation temperature at their designated operating pressure.

1.3 Objectives

The main objectives of this Master's project will be to understand how sloshing affects the thermodynamic response in an LNG fuel tank. Primary objectives in order of importance:

1. Understand how sloshing affects temperature and pressure in the tank.
2. Find heat transfer between liquid-vapour interface during sloshing.
3. Replicate results in simulation model (20-sim).

In addition, several secondary objectives has been introduced over the course of the thesis work:

- Study the effect of heat compensation during the experiments, i.e. maintaining heat flow to the system during sloshing.
- Calculate heat transfer coefficient between the tank and its surroundings.
- Measure capacity and calculate efficiency of the electrical heater.
- Identify and calculate the energy balance in the system.

1.4 Scope and Limitations

In order to simplify the experiments, water has been used as testing medium, due to it being both easily available and significantly easier to handle than LNG, which would have required a complicated testing procedure in order to keep it sufficiently cooled and pressurized. Water does have completely different physical properties compared to LNG, but these experiments are primarily conducted to observe the physical process.

As it is not possible to see inside the tank during the experiments, sloshing results from a smaller, transparent plastic tank has been used to illustrate parts of the sloshing regime, hoping to make it possible to understand what type of sloshing affects the system properties the most, as well as how the wave motion behaves.

For the calculations, it has been assumed that there is no presence of air inside the tank, only saturated vapour. As it is hard to control the amount of air inside, it was decided to disregard

the presence of air completely. An average temperature of both vapour and liquid has often had to be assumed, due to the variation of temperature in the different layers of vapour and liquid.

Chapter 2

Experimental Work

2.1 Setup of Experimental Rig

An insulated tank has been designed and built in the laboratory at NTNU Aalesund. This tank has been expanded to include piping in and out of a heating element, contained within a small steel container; hydrostatic pressure controls the level of the water within. The tank is placed on a sloshing rig previously built in the university laboratory; the sloshing motion is initiated through an electric motor controllable from a computer in the laboratory. In addition, both an angle sensor and a strain cell are installed, making it possible to measure both the angle of the rig during the sloshing experiments as well as the force required to initiate and maintain the motion. Figure 2.1 shows very simply the main arrangements of the rig. As one can see, the platform creates a rotational motion around the transverse axis of a ship.

Finding how temperatures on different levels of the tank behave during the experiments is integral in pursuit of the data required. Thus, a temperature probe has been created, setting up 13 thermocouples on different heights inside the tank, as shown in Figure 2.2, making it possible to measure how the temperature develops both in the vapour and in the water. The thermocouples are type T, which has a temperature range from -250°C to 350°C (Omega (2017)). In addition, an HBM P8AP absolute pressure transducer has been coupled to an HBM-box, in order to record absolute pressure during the experiment. The transducer has a strain-gauge sensor, with an accuracy of 0,3% (HBM (2017)). Thus it is possible to see at all times how the pressure match the temperature within the tank. An overview of the instrumentation used in

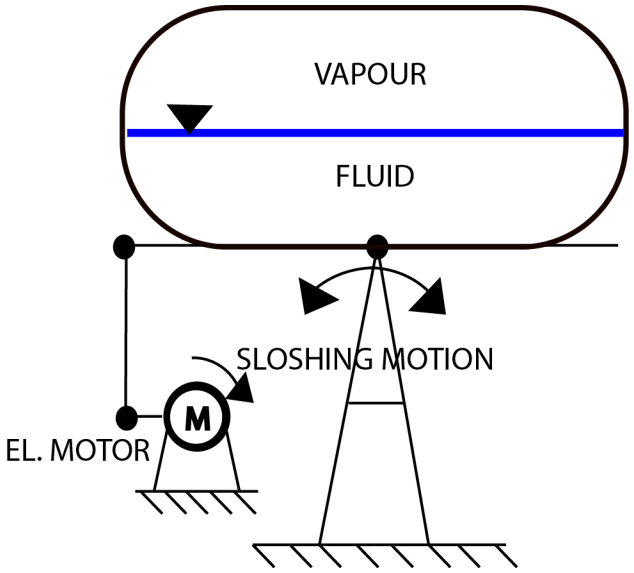

Figure 2.1: Illustration of sloshing rig

the experiments is shown in table 2.1.

Table 2.1: Experiment instrumentation

Device	Type	Range	Error
Temperature sensor	Thermocouple type T	-250-350 [°C]	±1.0[°C]
Pressure sensor	P8AP	0-20 [bar]	0.3%
Heating element	Høiax	0-3000 [W]	-
Power supply	Philips 2422 530 05401	0-260 [V]	-
Electro-motor	MAC800-D2	750 [W] @ 3000 RPM	±0.5%

All of the sensors have not been used at the same time in every experiment, as it would result in a rather unnecessary amount of data. As one can see in Figures 2.2 and 2.3 they are placed at various levels within the tank, giving the ability to choose which sensors to use dependent on e.g. the filling level of the tank. The initial experiments will be run with approximately 50 % filling level, with sensors 1, 2, 4, 6, 7, 8, 10, 12 and 13 activated. A filling level of 50 % is at the height of sensor no. 7. Unfortunately, sensor no. 8 did not work properly in the experiments conducted in sections 3.1 and 3.2, and has therefore been excluded from the result plots. Figure 2.4 shows main dimensions of the tank, created from a provided 3D-model.

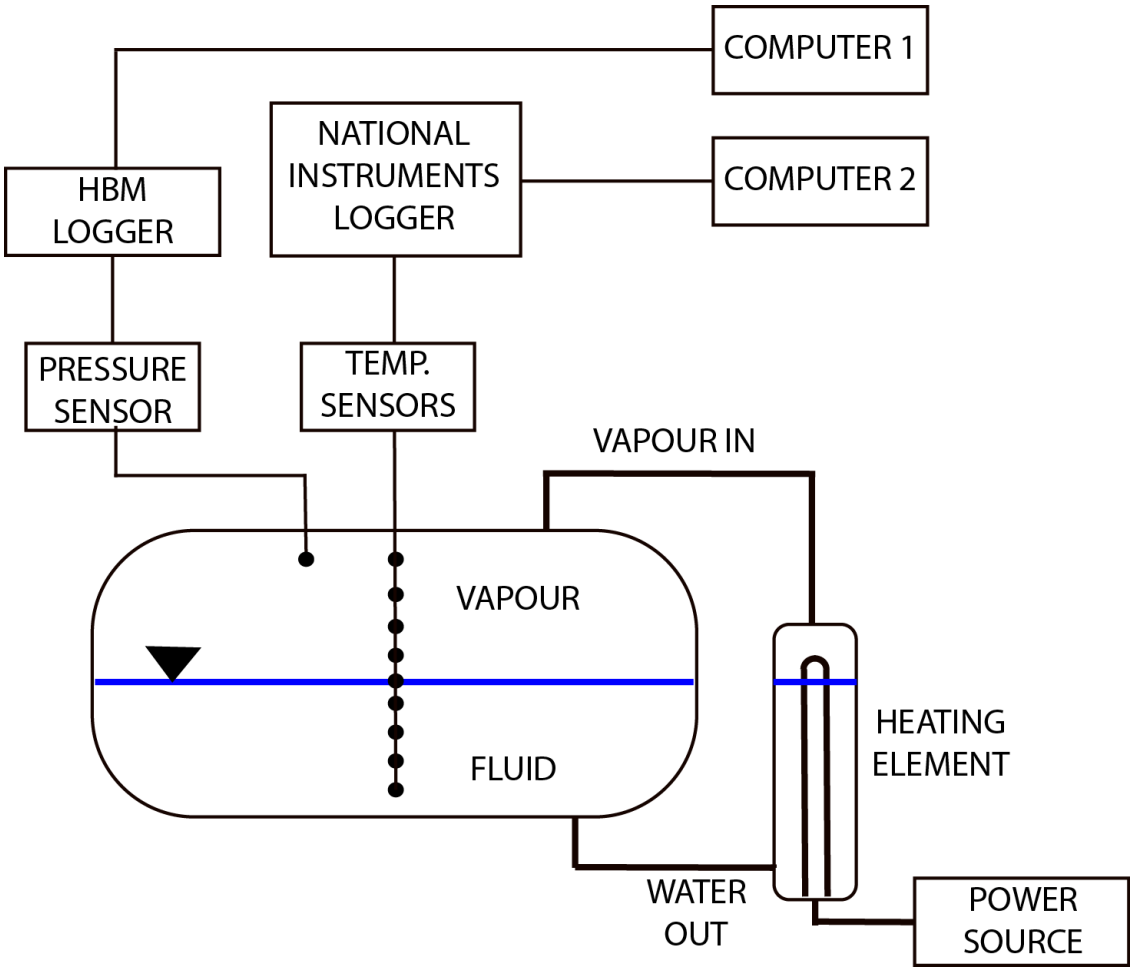

Figure 2.2: Experiment setup

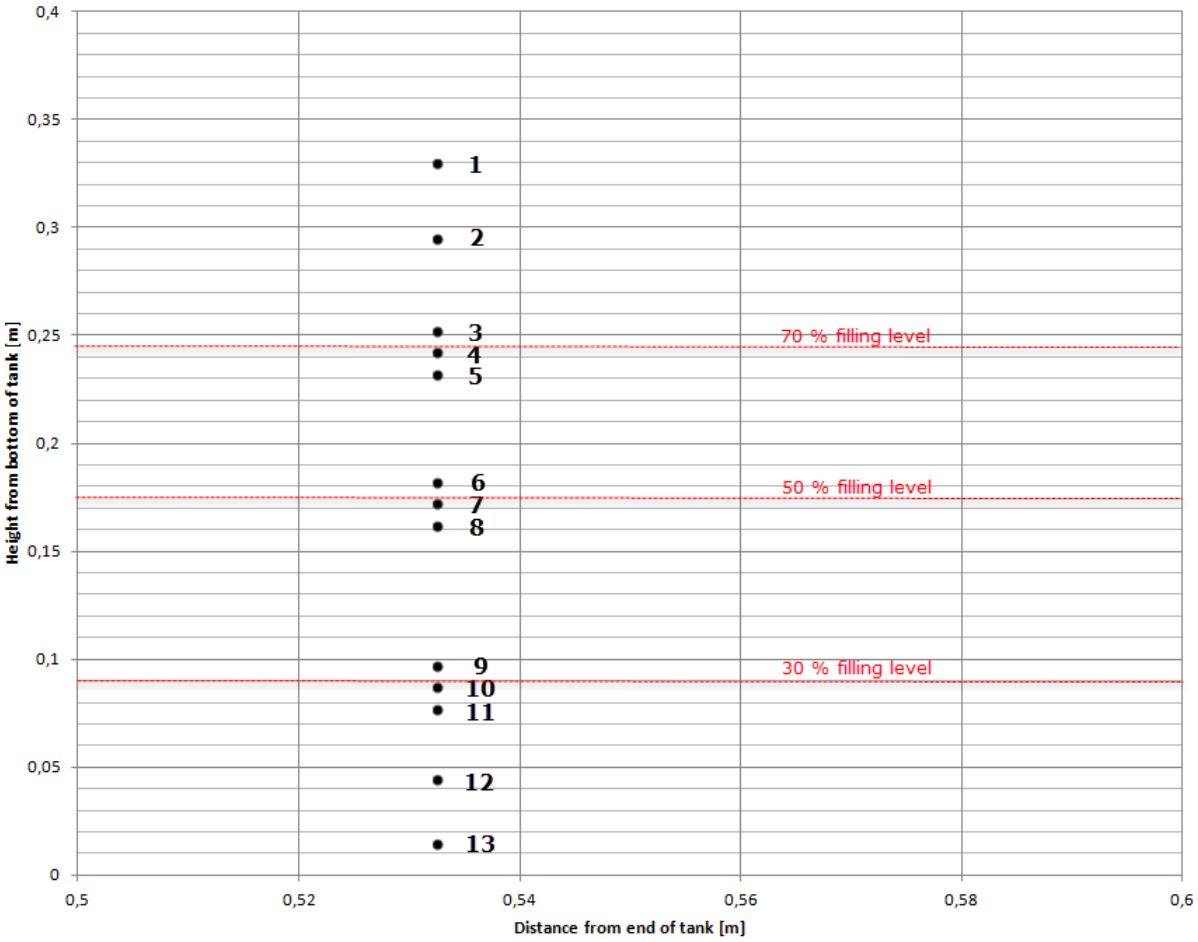

Figure 2.3: Temperature sensor overview

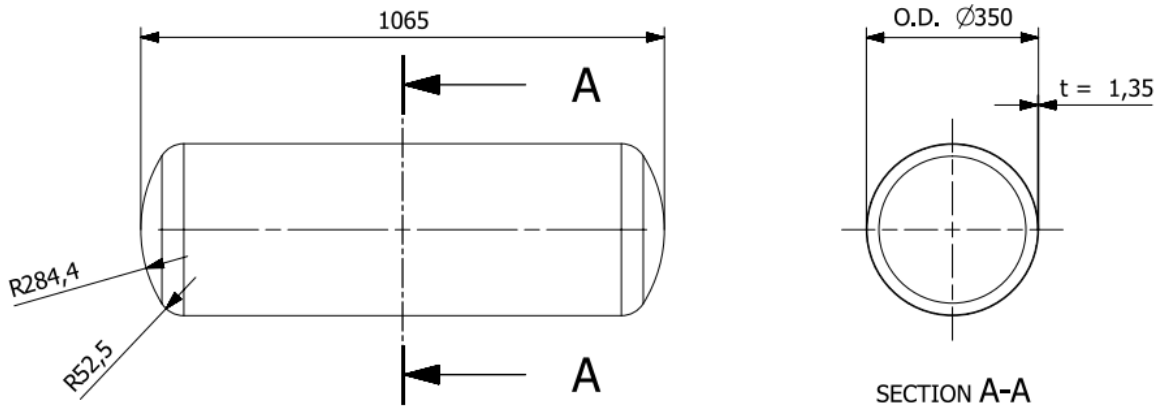

Figure 2.4: Tank main dimensions

2.2 Experiment Procedure

Before the experiments can be conducted, the water in the tank is heated from approximately 15°C to 120°C. This is a time consuming task, which starts with the heater being turned on, and subsequently heating the water. The power supply is limited to 1460 W, as the fuse have a tendency to break when subject to higher electrical power. To increase the temperature in the system as efficiently as possible, sloshing is utilized to transfer the heat energy from vapour to liquid. This pattern is repeated every time the pressure in the system reach 3 bar absolute pressure, making the experiment safer as well. In order to remove air from the tank, the tank is left open during the start of the heating process. The tank is then closed once the temperature of all the non-submerged sensors show close to 100°C. Figures 2.5 and 2.6 illustrates a typical system heating process over time, where the latter shows well how the liquid temperature increases through sloshing initiation.

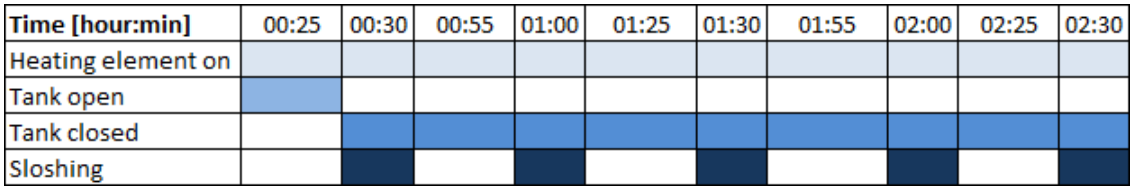

Figure 2.5: System heating process

Once the test medium's temperature has reached 120°C, and the absolute pressure inside the tank is 3 bar, the experiments can be conducted. As shown in figure 2.7, the experiments do take some time as the sloshing results in a higher liquid temperature, which subsequently needs to be cooled down before another test can be performed. The different tests need to have close-to-identical initial conditions, hence the importance of having as much saturated vapour inside as possible. Small amounts of air has to be assumed nonetheless. Tables from Moran and Shapiro (2006) shows that saturated water vapour holds a temperature of 133,6°C at 3 bar absolute pressure. Initial testing showed that the presence of air inside the tank resulted in a lower temperature than saturated vapour would hold at the given pressure.

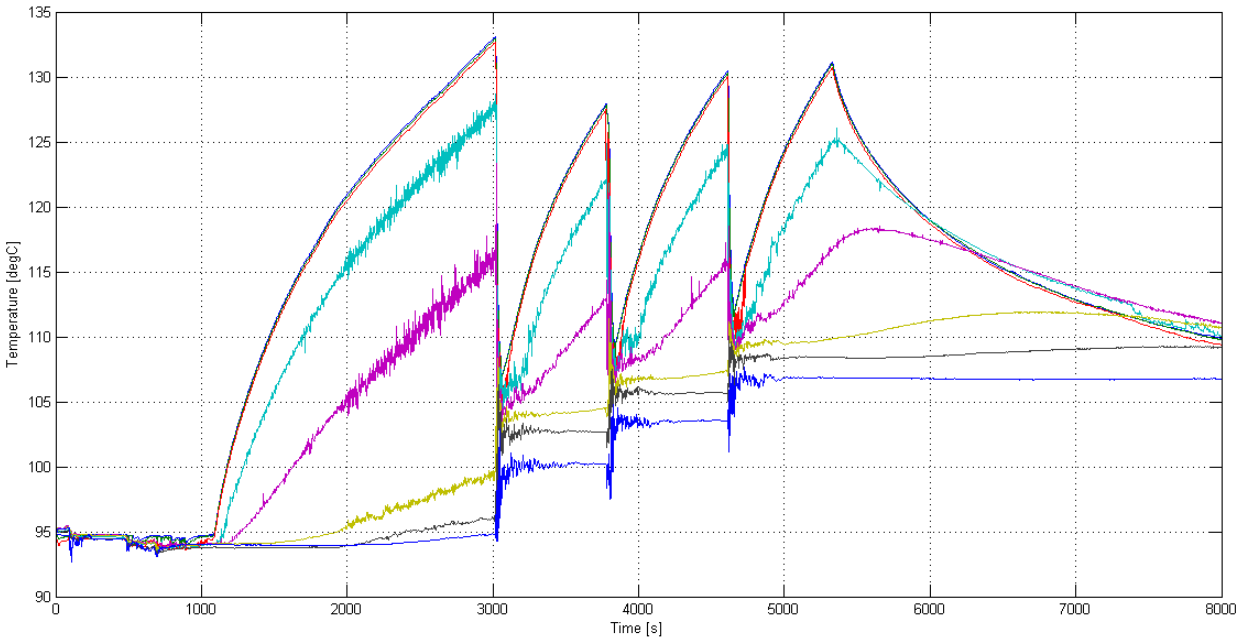

Figure 2.6: Plot of a typical heating process

Time [Hour:min]	00:10	00:15	01:00	01:10	01:15	02:00	02:10	02:15
Heating element on								
Sloshing								
Cooling								

Figure 2.7: Experiment process

Chapter 3

Experimental Results

3.1 System Heat Loss

Initial experimental work started with getting to know the system, e.g. heating the system and letting it cool down, thus finding the heat loss of the system; how fast it reacts to a change in heat input and how much heat it loses to its surroundings. In addition one can see how heat transfer between the liquid-vapour interface will behave.

The heat loss of the system was found through heating of the tank, and subsequent cool down by switching off the heating element. When temperatures of gas and liquid are equal, the proceeding loss is what goes out to its environment. As one can see in figure 3.1, the temperature of gas and liquid are close to equal after approximately 2 hours; the proceeding drop in temperature in the system is due to heat loss to the surroundings. The rate of energy transfer to the surroundings can be expressed through:

$$\dot{Q}_{loss} = U * A_{tank} * (T_{tank} - T_{surroundings}) \tag{3.1}$$

$$\dot{Q}_{cooling} = \sum m * C_v * \frac{dT}{dt} \tag{3.2}$$

Equation 3.1 being equal to equation 3.2, it is possible to solve for the heat transfer coefficient:

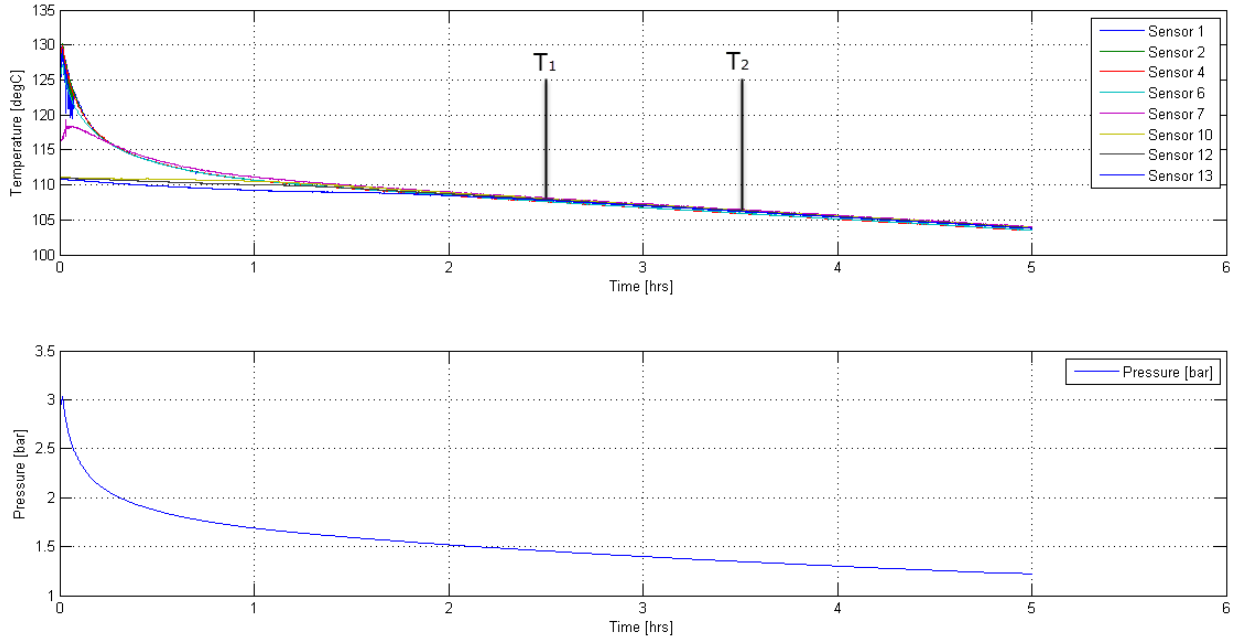

Figure 3.1: Tank cooling over a 5 hour period

$$\dot{Q}_{loss} = \dot{Q}_{cooling}$$

$$U * A * (T_{tank} - T_{surroundings}) = \sum m * C_v * \frac{dT}{dt}$$

Which gives:

$$U = \frac{\sum m * C_v * \frac{dT}{dt}}{A * (T_{tank} - T_{surroundings})} \tag{3.3}$$

Calculating total mass in the tank, assuming total mass of water and vapour to fill 50% of the tank volume. Also neglecting heat loss from water in pipe and in heating element container:

$$\sum m = 0,5 * V_{tank} * \rho_{water}$$

The main issue of calculating the heat conducted from this tank to its environment is due to the matter of its shape, making it a complicated affair to calculate the area. For simplicity, the area is therefore found by measuring the 3D-model. Several assumptions are made, as shown in table 3.1 below. Density of water at approximately 380 K as found in Moran and Shapiro (2006).

Table 3.1: Heat loss calculation parameters

$A_{tank}[m^2]$	$V_{tank}[m^3]$	$\rho_{water}[kg/m^3]$	$m_{water}[kg]$	$Cv_{water}[J/kgK]$	$T_{surr.}[K]$	$T_1[K]$	$T_2[K]$
2.48	0.1	960	48	4200	293	380.75	379.55

Heat transfer coefficient from tank to its surroundings from equation 3.3 is then:

$$U = 0.31 \frac{W}{m^2 K}$$

Thus, it is possible to calculate heat transfer from the tank to its surrounding by use of equation 3.1.

3.2 Heater Efficiency

Finding the amount of water the system was able to evaporate was important, therefore the mass flow was measured at different effects. By keeping a bucket filled with water at the same level as it would have been at 50 % filling level within the tank, it was possible for find the amount of water being evaporated by measuring the remaining mass of water in the bucket with a scale every minute for a period of at least 10 minutes. Thus, it was also possible to find the approximate efficiency of the heater. The electrical power was measured with a voltmeter coming out from the power source. Setup of the experiment is shown in figure 3.2 below.

From the results found in this experiment, as shown in table 3.2, it is possible to find the effect necessary to vaporize the measured flow, utilizing the latent heat of evaporation for water, assumed to be $\Delta hfg = 2257 * 10^3 J/kg$ for this case.

$$\dot{Q}_{latent} = \Delta hfg * \dot{m} \tag{3.4}$$

$$\dot{Q}_{heat} = \dot{m} * C_p * \Delta T \tag{3.5}$$

Where:

$$\Delta T = T_{boil} - T_{waterin}$$

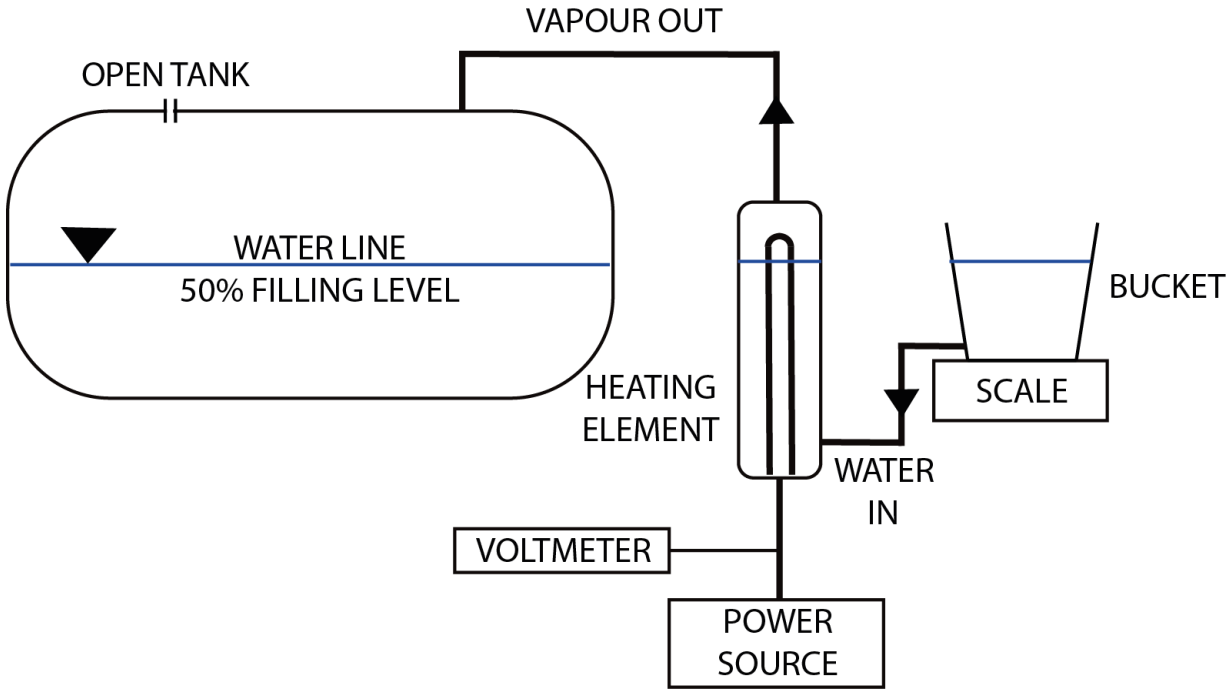

Figure 3.2: Setup of heater experiment

$$\eta = \left(\frac{\dot{Q}_{total}}{Power_{electrical}}\right) \tag{3.6}$$

Where:

$$\dot{Q}_{total} = \dot{Q}_{vaporize} + \dot{Q}_{heat} - \dot{Q}_{loss}$$

From equation 3.4 one can calculate the power necessary to evaporate the measured flow. The data was measured once a steady state had been achieved, which should exclude the power required to heat the entire contents of the tank, leaving only the water coming in to the container, which needs to be heated from approximately 15°C to 100°C. From equation 3.5 one finds the effect needed to heat a certain flow of water by utilizing the specific heat capacity of the water at constant pressure, which as an open system, this is assumed to be. Equation 3.6 calculates the efficiency of the heater.

As one can see from table 3.2, the efficiency is ranging from 83,8% to 95,2%, with two assumed losses; loss of electrical power through the wires, and heat loss to environment. In addition, the container of the heating element is constructed in such a way that the whole element is not submerged at 50% filling level. Thus, the full effect will not be used to heat and vaporize

Table 3.2: Heater efficiency.

$\text{Power}_{electrical}[W]$	Flow [kg/s]	$\dot{Q}_{vaporize}$ [W]	$\dot{Q}_{heat}$ [W]	$\dot{Q}_{loss}$ [W]	η[%]
570	$1{,}83\times10^{-4}$	413	64,6	92,4	83,8
982	$3{,}37\times10^{-4}$	761	119,9	101,1	89,7
1461	$4{,}91\times10^{-4}$	1105	172,9	183,1	87,5
2019	$7{,}37\times10^{-4}$	1663	260,0	96,0	95,2

the water. This can also explain why using a higher electrical power results in higher efficiency; the boiling water rises in level, thus utilizing more of the heating coil.

The results gathered here can be used for calculations even when there is pressure in the system. If the tank was closed there would quickly be a counter-pressure acting on the vapour, but this pressure would also be acting on the liquid in the tank, providing equilibrium.

3.3 Sloshing at 50% Filling Level

Through sloshing at different frequencies one can observe how the severity of the sloshing affects the pressure drop as well as the mixing of the temperature. These experiments were conducted in order to observe how severe wave motion can affect the contents of the tank. In tables 3.3 and 3.4 one can see the initial conditions and results from the experiment, respectively. Sloshing was run for 20 periods at different frequencies, thus representing a clearer picture of how the different conditions would affect the system. 10 different sloshing cases were included, period duration ranging from 1.75 seconds to 4.00 seconds. In addition, a case was included where no tank excitation was initiated, for reference. Sloshing parameters for the reference results are referred to as 'not applicable' (N/A).

Mixing time is considered as the time it takes for the temperature registered by all sensors to be close-to-equal, i.e. the time it takes for the tank's contents to mix together. In cases 3-10 the mixing time exceeded the duration of the sloshing test, indicating by the temperature plots that it will take a significant amount of time before this happens.

As one can see from figure 3.3, the difference in pressure drop is significant. Case 1-3, and to some extent case 4, show severe pressure drop happening shortly after sloshing is introduced. In contrast, case 5-10 shows more of an even pressure drop. Still, it's easy to see the significance

Table 3.3: Initial conditions sloshing at 50% filling level

Case	$T_{Gas}[K]$	$T_{Liquid}[K]$	$\Delta T_0[K]$	$\lvert p_0 \rvert [bar]$
1	405.95	393.46	12.49	3.04
2	405.88	393.09	12.79	3.00
3	406.08	393.35	12.73	3.02
4	405.31	393.08	12.23	3.01
5	405.37	393.14	12.23	3.02
6	406.05	393.59	12.46	3.06
7	405.85	393.02	12.83	3.02
8	405.80	393.05	12.75	3.02
9	405.88	393.24	12.64	3.04
10	406.16	393.35	12.81	3.06
11	405.80	393.08	12.72	3.02

Table 3.4: Results of sloshing cases 1-11 at 50% filling level

Case	Period [s]	Frequency [1/s]	Duration [s]	$\Delta T_G[K]$	$\Delta T_L[K]$	$\Delta p[bar]$	$\lvert dp/dt \rvert_{max}[bar/s]$
1	1.75	0.57	35	-10.57	1.87	-0.82	0.78
2	2.00	0.50	40	-11.51	1.23	-0.87	0.86
3	2.25	0.44	45	-11.47	1.16	-0.88	0.72
4	2.50	0.40	50	-10.87	0.87	-0.84	0.47
5	2.75	0.36	55	-7.85	-0.16	-0.66	0.21
6	3.00	0.33	60	-5.67	0.09	-0.49	0.07
7	3.25	0.31	65	-6.51	-0.08	-0.57	0.06
8	3.50	0.29	70	-5.59	-0.01	-0.48	0.06
9	3.75	0.27	75	-4.93	0.03	-0.44	0.05
10	4.00	0.25	80	-4.77	-0.07	-0.43	0.04
11	N/A	N/A	80	-2.95	-0.03	-0.25	0.02

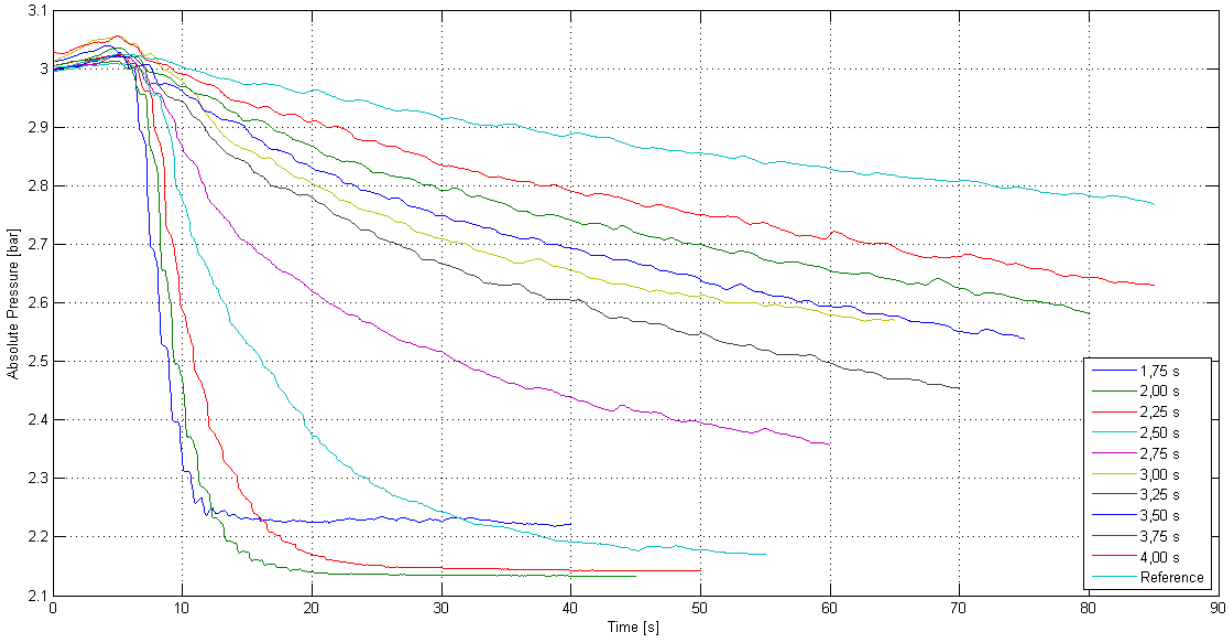

Figure 3.3: Pressure plot case 1-11 at 50% filling level

the introduction of sloshing has on the pressure in the tank. An unexpected result to see is that the pressure drop in case 1 is lower than case 2-4, suggesting that a higher frequency of sloshing does not always result in higher pressure drops.

Figure 3.4 shows how the temperature within the tank responds to sloshing at a period of T=1.75 seconds, or frequency f=0.57 Hz. An issue with the logger resulted in the plots looking a bit odd during these tests; this was presumably due to the sensors likely not being able to register values at a frequency of 20 Hz, thus resulting in 10 equal values every 0.5 seconds.

From the temperature plots in figures 3.4 and 3.5 one can see clearly that the sloshing results in temperature mixing within the tank, and also presumably complete condensation of all vapour inside the tank. The amount of condensed vapour, Δm, can be calculated from the pressure drop, Δp. As can be seen in table 3.4, the sloshing cases with periods ranging from T=1.75 seconds to T=2.50 seconds are the only times a clear increase in liquid temperature is evident. This indicates that only severe sloshing creates enough mass transfer for a significant amount of the vapour to condensate.

Both figures 3.6 and 3.7 show that there is not enough motion inside the tank for the tem-

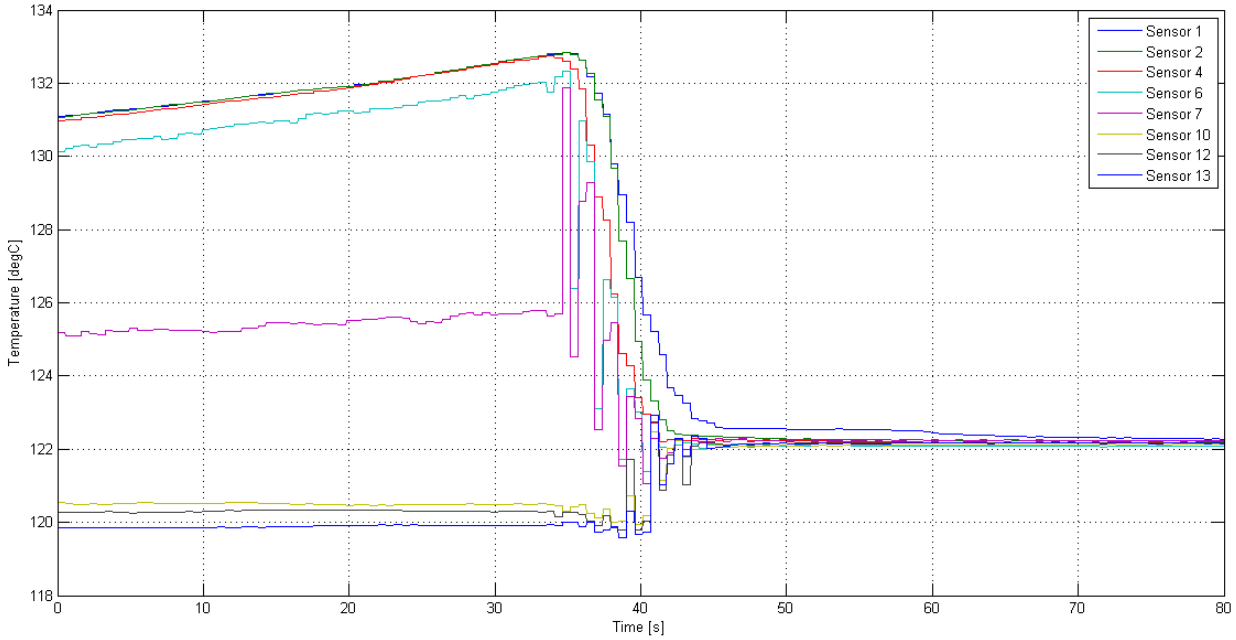

Figure 3.4: Temperature plot case 1, T=1.75 s at 50% filling level

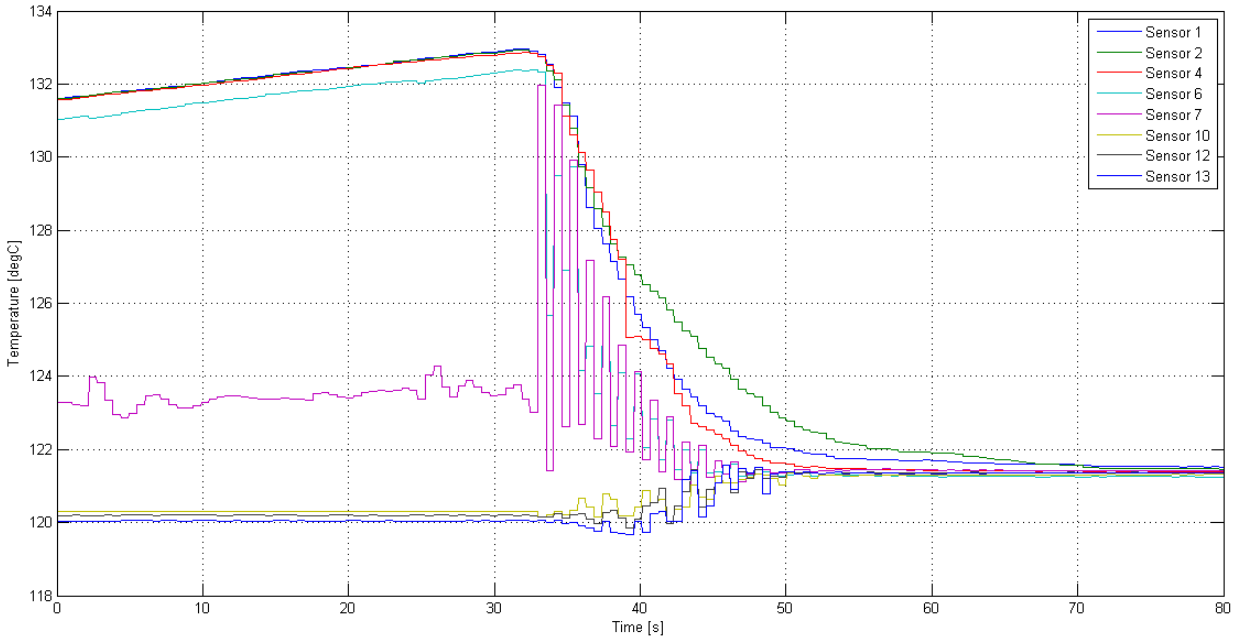

Figure 3.5: Temperature plot case 3, T=2.25 s at 50% filling level

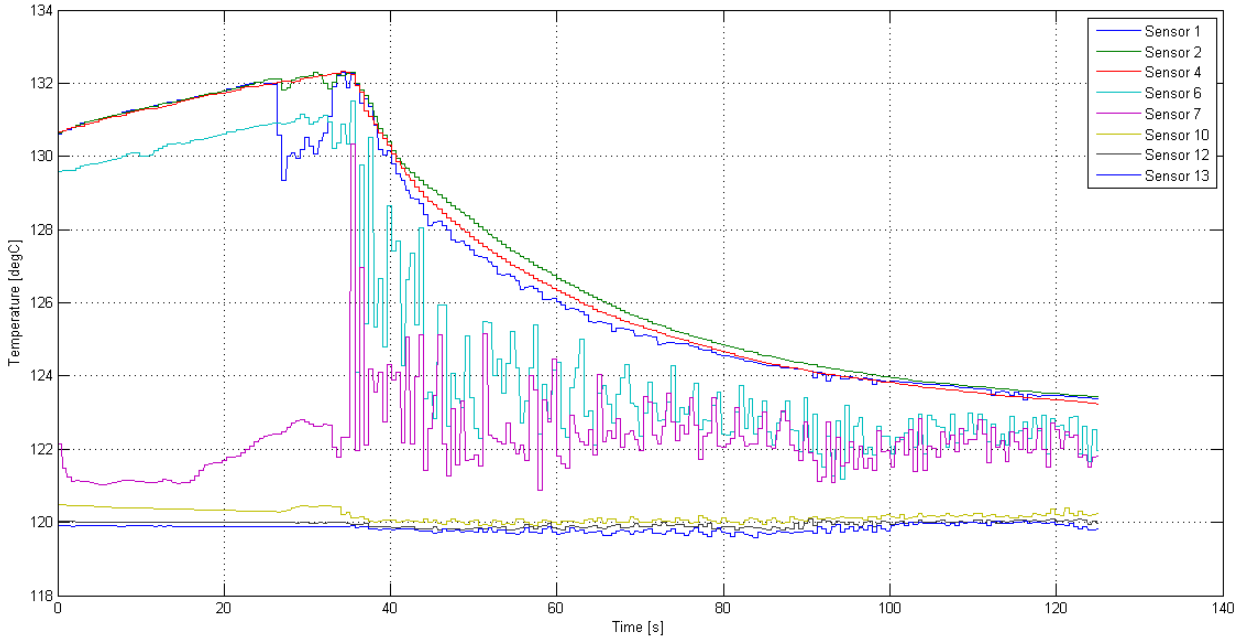

Figure 3.6: Temperature plot case 6, T=3.00 s at 50% filling level

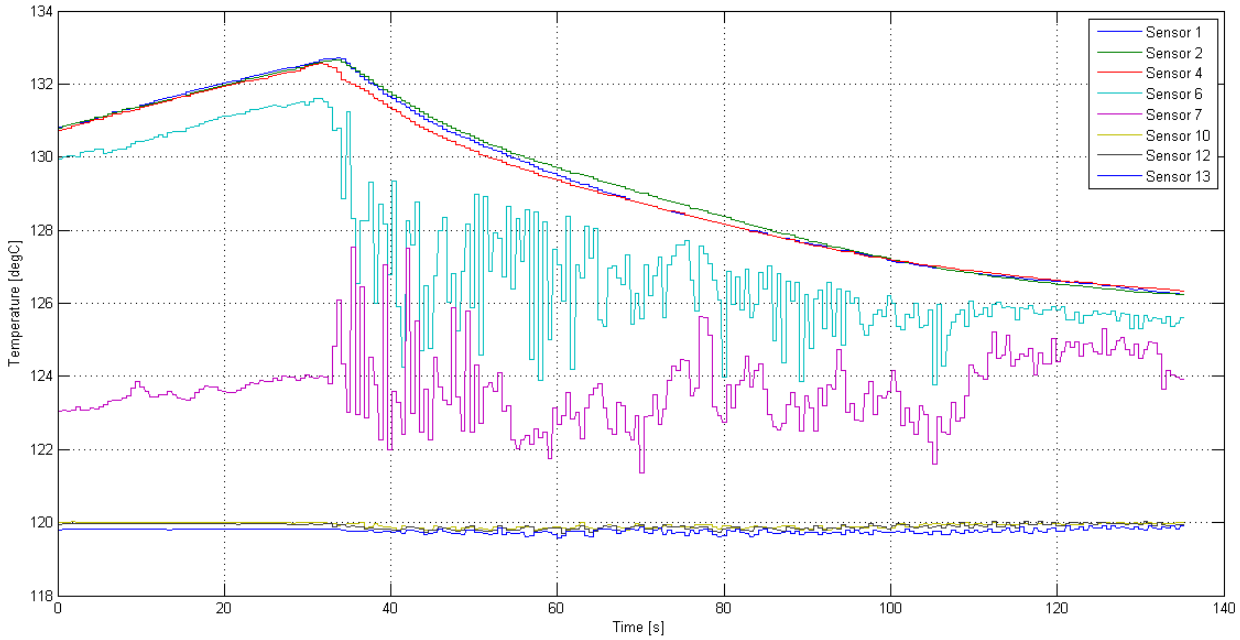

Figure 3.7: Temperature plot case 8, T=3.50 s at 50% filling level

peratures to mix. One can see from the plots for sensors 6 and 7, which are clearly oscillating. This is due to their position, as they are located just above and on the surface, respectively, as can be seen in figure 2.3. Such an oscillation in temperature is likely due to the interface oscillating, but also the sample speed of the thermocouples, not recording temperatures with a high enough speed to keep up with the oscillation.

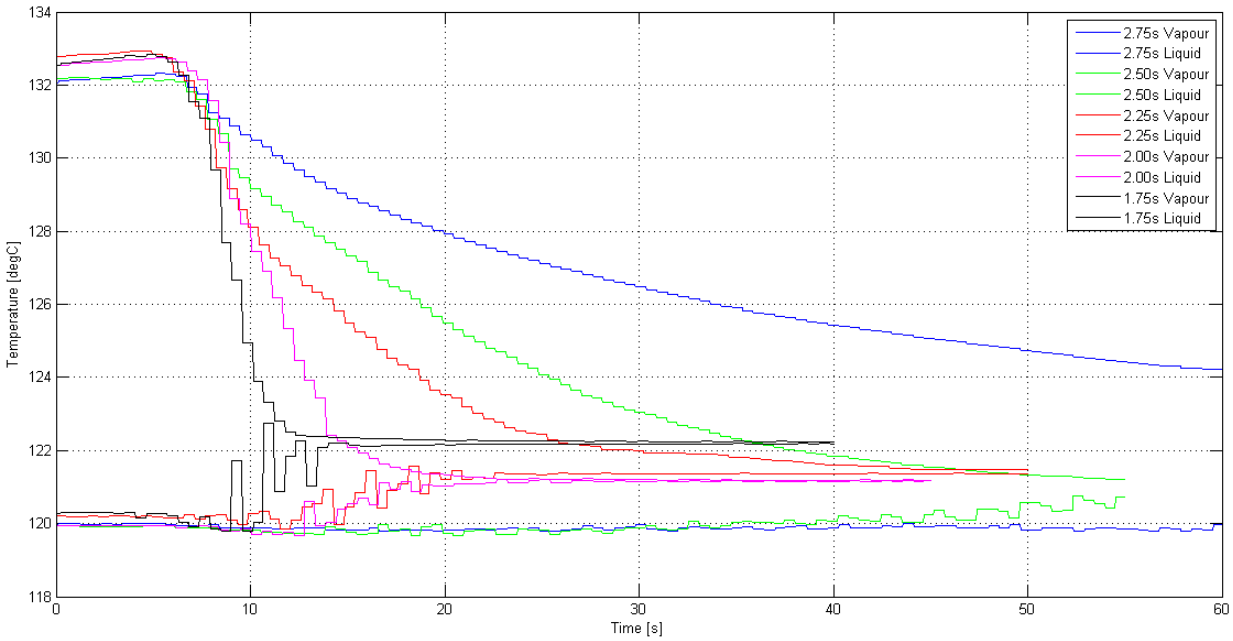

Figure 3.8: Temperature plot case 1-5 at 50% filling level

Case 1-5 from table 3.4 are shown in figure 3.8. Sensors 2 and 12 were used for this plot, both placed in positions to measure temperature of vapour and liquid respectively, as can be seen in figure 2.3. They were plotted in order to show the distinct difference the frequency of the sloshing had on the heat transfer, especially case 1-3, which rapidly transfers energy from vapour to liquid.

Case 6-10 are different, as the tank motion mostly result in oscillations of the liquid temperature. The vapour temperature drops by as much as 6.51°C, which should indicate that some energy is transferred, but it is not noticeable on the liquid temperature within this time scope.

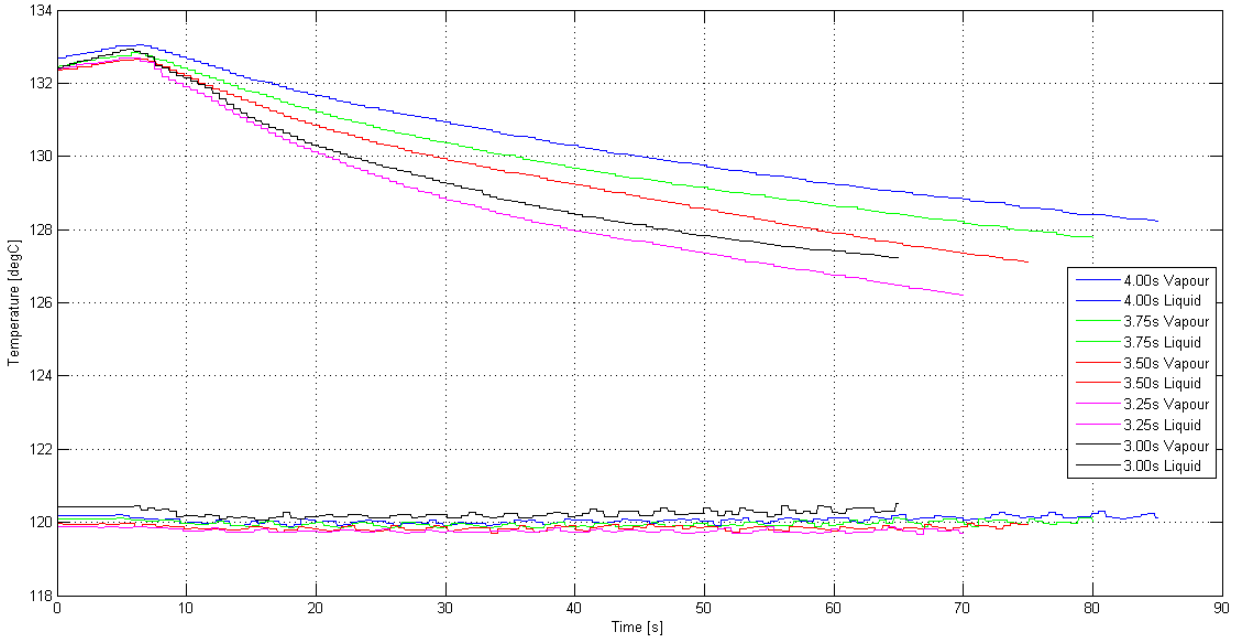

Figure 3.9: Temperature plot case 6-10 at 50% filling level

3.4 Sloshing at 50% Filling Level - Heat Compensation

The previous tests shown in Figures 3.3 and (insert figure 4 of temperature plot) was run with the heating element switched off. It was the plan from the start of the experimental work to attempt to compensate the pressure loss by use of the heating element. A natural start was to compare a selection of the previous tests with the heating element on. An electrical effect of 1460 W maintained during sloshing, comparing with the results without heating.

Table 3.5: Initial conditions sloshing at 50% filling level with heating element on.

Case	$T_{Gas}[K]$	$T_{Liquid}[K]$	$\Delta T_0[K]$	$\|p_0\|[bar]$
1	406.04	393.56	12.48	3.05
2	405.77	393.28	12.49	3.02
3	405.61	392.87	12.74	3.01
4	405.76	393.09	12.67	3.02
5	406.45	393.42	13.03	3.07
6	406.31	393.57	12.72	3.07

One can clearly see the impact of having the heating element on during the tests, especially evident at a sloshing period of T=4.00 seconds, where the pressure keeps rising despite tank ex-

Table 3.6: Results of sloshing case 1-6 at 50% filling level with heating element on

Case	Period [s]	Frequency [1/s]	Duration [s]	$\Delta T_G[K]$	$\Delta T_L[K]$	$\Delta p[bar]$	$\lvert dp/dt \rvert_{max}[bar/s]$
1	1.75	0.57	35	-9.76	2.48	-0.77	0.73
2	2.00	0.50	40	-10.84	1.32	-0.83	0.89
3	2.50	0.40	50	-9.59	0.67	-0.78	0.50
4	3.00	0.33	60	-2.61	-0.09	-0.22	0.09
5	3.50	0.29	70	-0.73	0.08	-0.05	0.04
6	4.00	0.25	80	0.63	-0.02	0.05	0.04

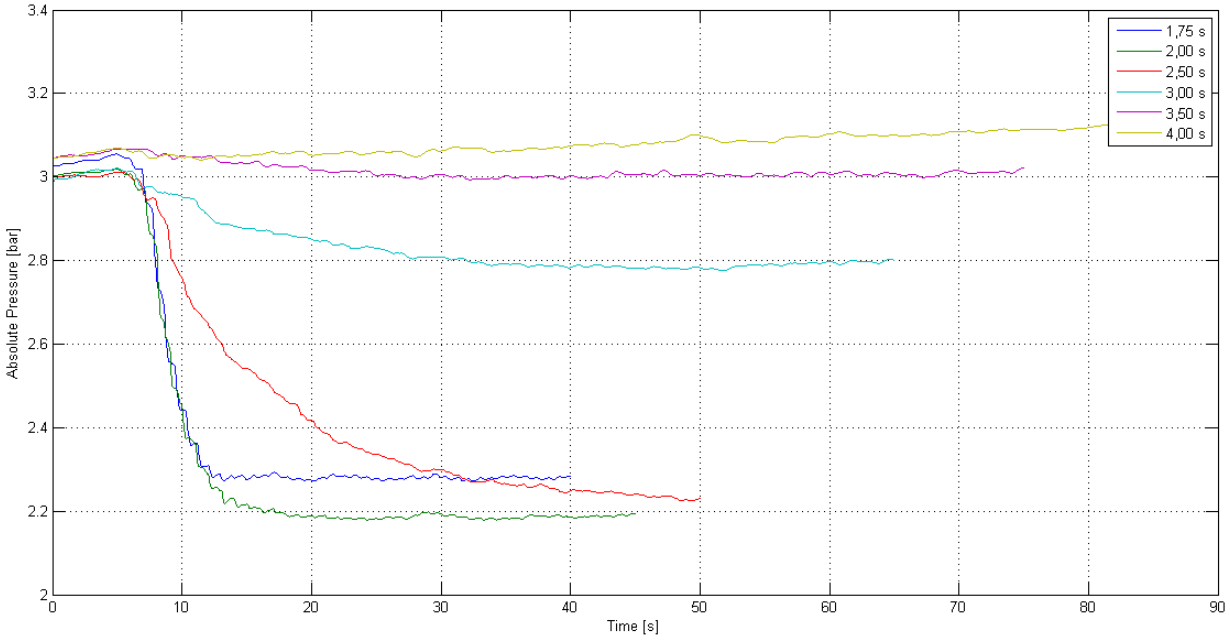

Figure 3.10: Pressure plot case 1-6 with heating element on at 50% filling level

citation. T=3.50 seconds seems very well balanced in terms of energy added from the heating element compared to energy transferred due to sloshing. Further, one can see from the results that the magnitude of the pressure drop is reduced compared to tests run without heat compensation. In this test one can also see that the pressure drop in case 1 is lower than case 2-3, which was also observed in figure 3.3.

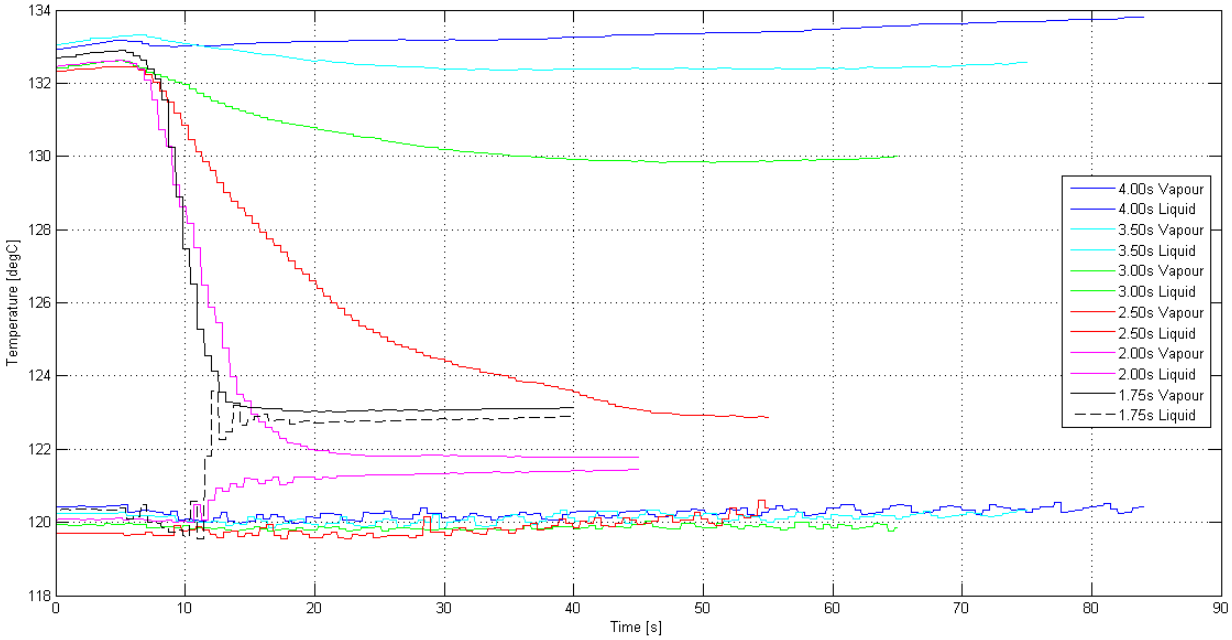

Figure 3.11: Temperature plot case 1-6 with heating element on at 50% filling level, sensor 2 and 12

3.5 Sloshing at 30% Filling Level

In the process of understanding what type of wave motion is the most severe, it was decided to conduct experiments where the filling level inside the tank was reduced from 50% to 30%. In order to not waste too much time by testing a huge amount of frequencies, the supervisor suggested four different frequencies which were of interest. These were directly scaled from a smaller, transparent sloshing tank.

Table 3.7: Initial conditions sloshing at 30% filling level

Case	$T_{Gas}[K]$	$T_{Liquid}[K]$	$\Delta T_0[K]$	$\|p_0\|[bar]$
1	405.83	393.22	12.61	3.01
2	405.96	393.89	13.07	3.01
3	405.79	392.87	12.92	3.01
4	405.99	394.11	11.88	3.02

What is interesting from these cases is the fact that the pressure drop profiles of all four tests are all very similar, maybe indicating that the fluid motion at such a low filling level is hard to vary. The frequencies tested in these experiments are of course not extremely different,

Table 3.8: Results of sloshing case 1-4 at 30% filling level

Case	Period [s]	Frequency [1/s]	Duration [s]	$\Delta T_G[K]$	$\Delta T_L[K]$	$\Delta p[bar]$	$\lvert dp/dt \rvert_{max}$
1	1.88	0.53	94.1	-10.03	2.46	-0.78	0.25
2	1.99	0.50	99.6	-10.30	2.58	-0.79	0.26
3	2.17	0.46	87.0	-10.00	2.58	-0.80	0.25
4	2.39	0.42	95.6	-9.60	2.25	-0.76	0.25

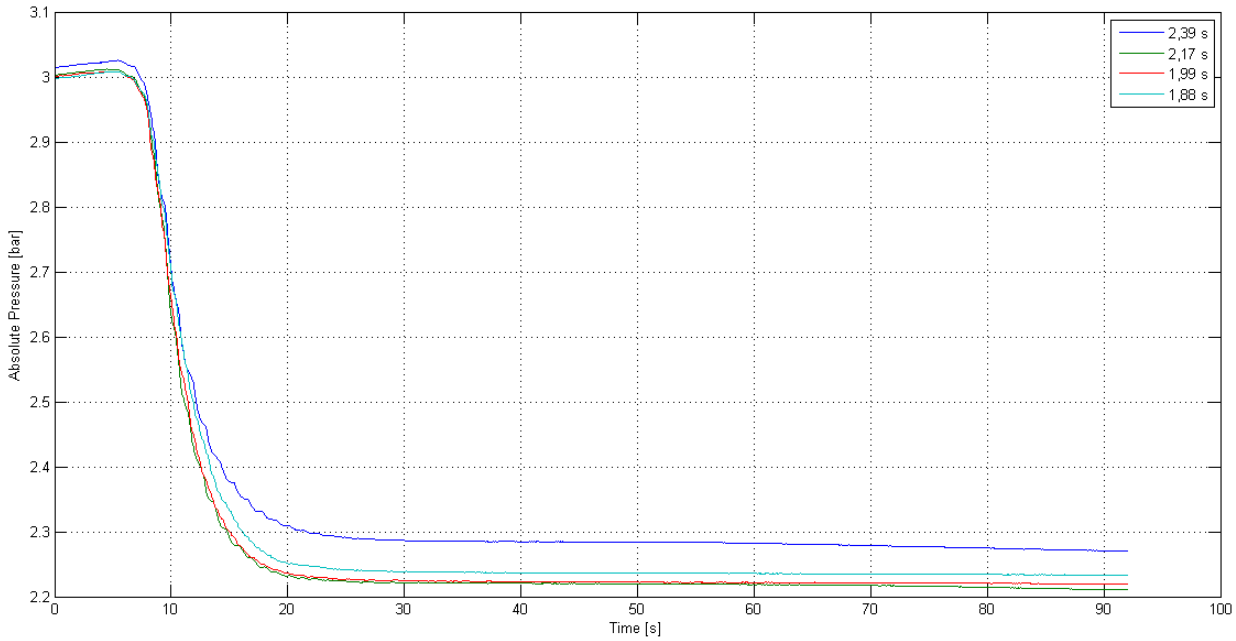

Figure 3.12: Pressure plot cases 1-4 at 30% filling level

but larger differences than the close-to-identical results seen in this experiment were expected. Pictures of the scaled frequencies that were tested in the transparent sloshing tank is shown in figures 3.13 and 3.14. The main difference observed from the illustrations are that while in figure 3.13, which is the slowest of the frequencies, the interface is hardly breaking up, except locally when rolling against the wall. Meanwhile, in the other three cases tested, here illustrated by figure 3.14, there is constant oscillation of the interface along with rapid crashing against the tank wall, causing liquid to splash up to the tank ceiling.

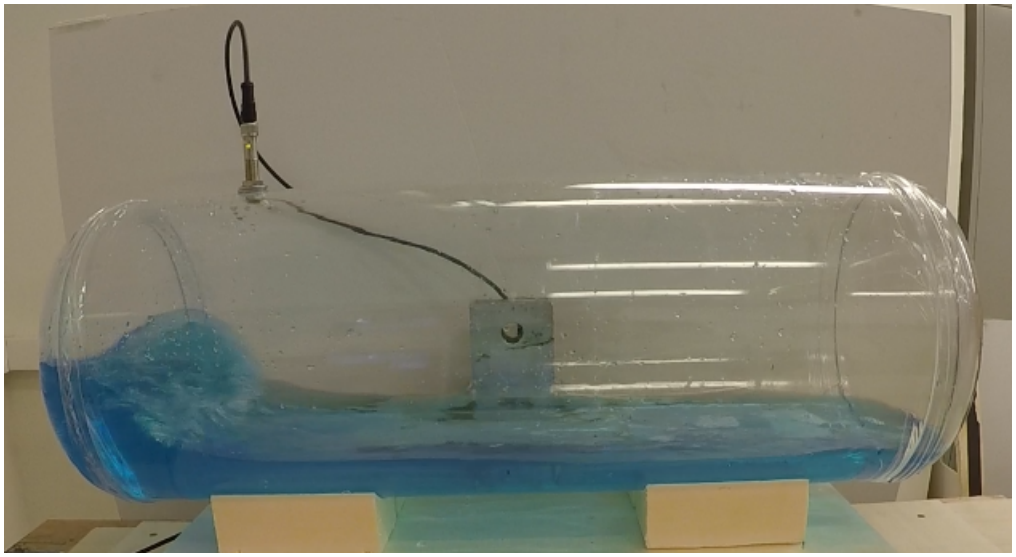

Figure 3.13: Sloshing at scaled period of T=2.39 s at 30% filling level in transparent sloshing tank (Grotle et al. (2016))

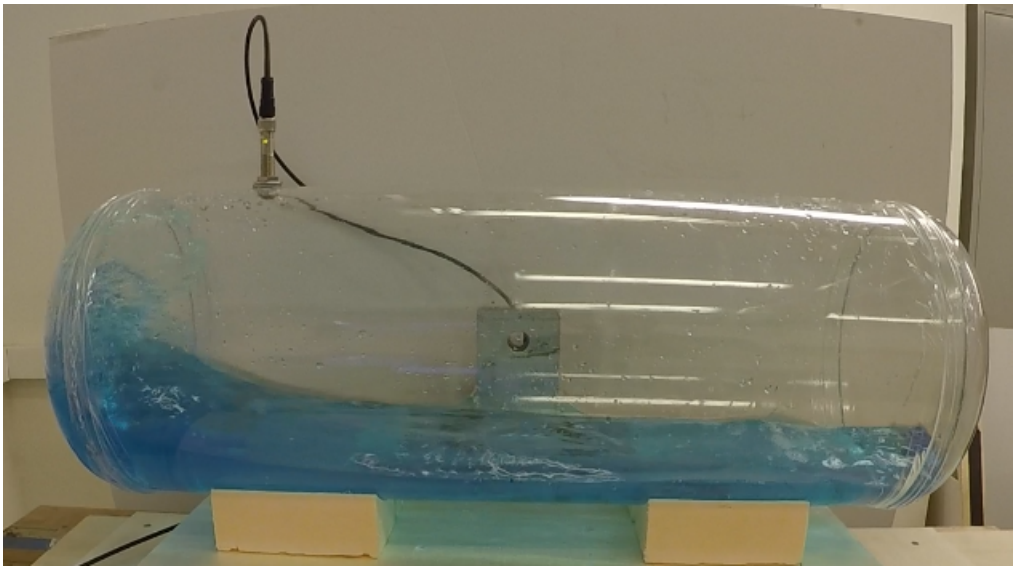

Figure 3.14: Sloshing at scaled period of T=1.99 s at 30% filling level in transparent sloshing tank (Grotle et al. (2016))

Chapter 4

Results and Analysis

4.1 Heat Transfer Over the Liquid-Vapour Interface

It has been shown from the results in Chapter 3 that sloshing increases energy transfer over the liquid-vapour interface. Here, it will be investigated the magnitude and rate of heat and mass transfer produced by sloshing. By neglecting any presence of air, calculating the mass of vapour can be done by use of the ideal gas law (equation 4.1) at set points during the sloshing experiments. Thus, it is possible to find the amount of vapour condensing during the experiment. A selection of results of interest will be used in these calculations, as found in tables 3.3 and 3.4.

$$pV = mRT \tag{4.1}$$

There are only 3 cases, as shown in figure 3.3, where the pressure reaches a bottom point. These are also the only cases where the temperature within the tank mixes properly, i.e. temperature of both vapour and liquid are close-to-equal. Thus, these are the only tests where the entire magnitude of energy transfer can be calculated, as it is not possible to know how much the pressure would have dropped had the sloshing continued further. An issue with calculating on these data, is the difference in values showed by the sensors at different levels in the tank. For the calculations, an average temperature in both liquid in vapour should be used, but as shown in figure 4.1, finding an average temperature is not so easy.

The horizontal lines within the cross-section of the tank represent the level of the sensor

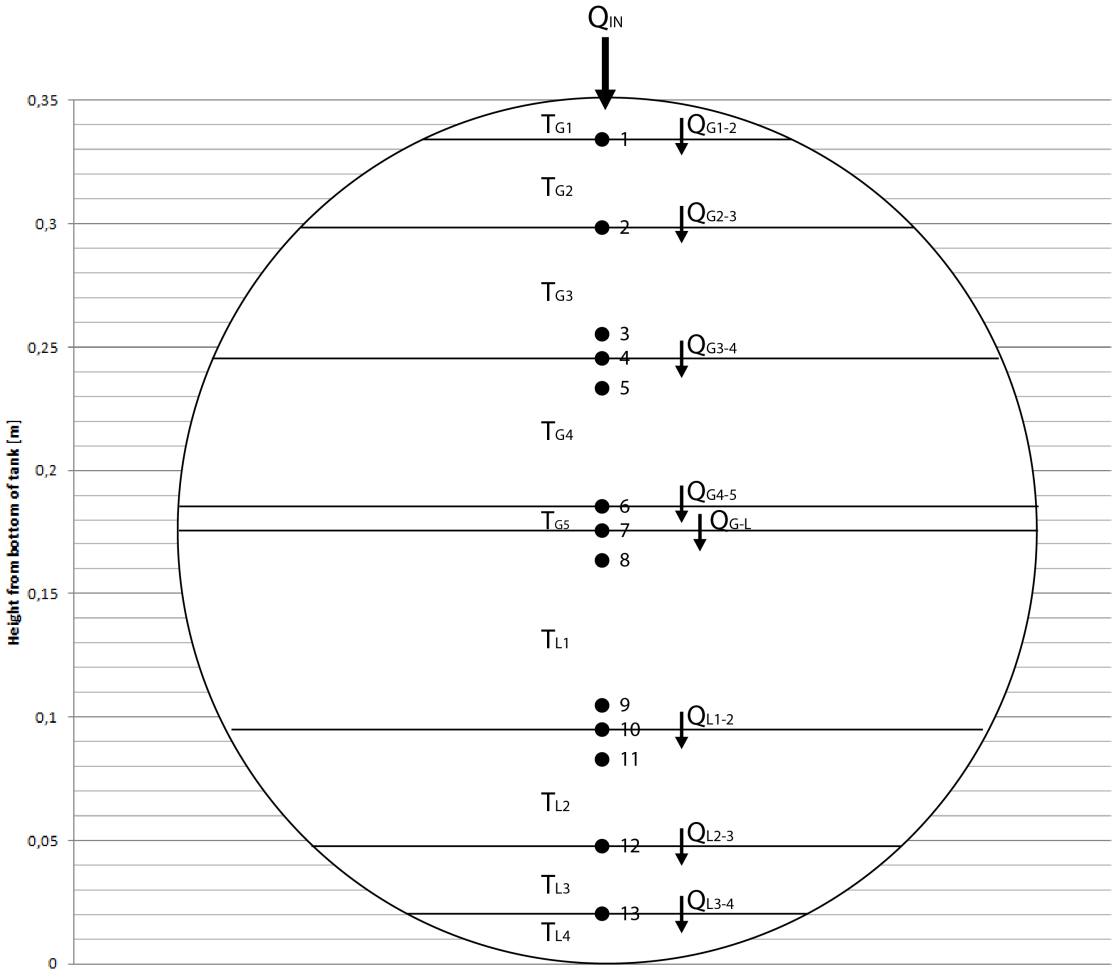

Figure 4.1: Heat flow in system during tests at 50% filling level

logging the temperatures during the experiments conducted at 50% filling level. As can be seen in the figure, the heat is transferred through the different layers of vapour and liquid, all with different amounts of mass. Therefore, finding a reliable average temperature for the calculations can be hard.

4.1.1 Magnitude of Heat and Mass Transfer

By use of equation 4.1 one can calculate the mass of vapour in the tank prior to and after sloshing has been performed. For this calculation, case 1 with a sloshing period of T=1.75 seconds will be used. The individual gas constant R can be calculated from the universal gas constant and the molecular weight of water (Moran and Shapiro (2006)):

$$R = \frac{\bar{R}}{M} = 461.5 \frac{J}{kgK}$$

$$m_1 = 0.081kg$$

$$m_2 = 0.061kg$$

$$\Delta m = m_2 - m_1 = -0.02kg$$

Total internal energy can be simplified to:

$$U_{tot} = U_G + U_L$$

Where:

$$U_G = m_G * u_G$$

$$U_L = m_L * u_L$$

Calculating for initial state, prior to sloshing:

$$U_{G1} = 0.081kg * 2543.6kJ/kg = 206.03 * 10^3 J$$

$$U_{L1} = 48kg * 504.49kJ/kg = 24.22 * 10^6 J$$

Calculating for final state, after sloshing:

$$U_{G2} = 0.061kg * 2531kJ/kg = 154.39 * 10^3 J$$

$$U_{L2} = 48.02kg * 511.45kJ/kg = 24.56 * 10^6 J$$

Change in internal energy in vapour and liquid:

$$\Delta U_G = -51.64 * 10^3 J$$

$$\Delta U_L = 344.31 * 10^3 J$$

Calculating how much change in temperature the change in internal energy in liquid would represent:

$$\Delta U_L = m_L * Cv_L * \Delta T_{L-calc}$$

$$\Delta T_{L-calc} = \frac{\Delta U_L}{m_L * Cv_L}$$

$$\Delta T_{L-calc} = 1.70K$$

Out of interest of the accuracy of the theory, the two remaining relevant cases are also calculated and compared to the results from the experiments, as shown in table 4.1.

Table 4.1: Calculation parameters and results for magnitude of heat transfer

$T_{slosh}[s]$	$\Delta m_G[kg]$	$\Delta U_G[kJ]$	$\Delta U_L[kJ]$	$\Delta T_{L-measured}[K]$	$\Delta T_{L-calc}[K]$
1.75	-0.02	-51.64	344.21	1.87	1.70
2.00	-0.021	-54.03	490.71	1.23	2.43
2.25	-0.022	-56.65	515.23	1.16	2.55

While the first calculation shows promise, there seems to be an error with the calculations. There is a possibility that including sensible heat would make it more accurate, although this has been neglected due to its presumed small contribution.

4.1.2 Rate of Heat and Mass Transfer

As mentioned above, for most of the cases tested, the pressure drop does not reach a bottom level in most of the tests. Thus, the rate of energy transfer will be calculated from set points on the pressure curve, assuming a linear profile within the scope. Otherwise the same considerations mentioned in Section 4.1.1 apply. The rate of mass transfer will be investigated, using ideal gas law (equation 4.1) to calculate change in mass. The rate of mass transfer can thus be calculated from:

$$\frac{dm_G}{dt} = \frac{m_{G2} - m_{G1}}{t_2 - t_1} \tag{4.2}$$

Further, the rate of energy transfer can be expressed as:

$$\frac{dU}{dt} = \frac{(m_{G2}u_{G2} - m_{G1}u_{G1}) + (m_{L2}u_{L2} - m_{L1}u_{L1})}{t_2 - t_1} \tag{4.3}$$

In addition to calculating the effect sloshing has on the rate of heat and mass transfer, the case with no tank excitation will be included, in order see the difference. Noted in table 4.2 as 'not applicable' (N/A).

Table 4.2: Results rate of heat and mass transfer

$T_{sloshing}[s]$	$\lvert dm_G/dt \rvert \times 10^{-4}[kg/s]$	|dU/dt| [J/s]
2.50	6.73	1388.11
3.00	3.34	689.48
3.50	2.68	553.20
4.00	1.91	396.06
N/A	1.09	225.08

As table 4.2 shows clearly, sloshing has a substantial impact on heat and mass transfer. Even with a slow sloshing period, e.g. T=4.00 seconds, the heat and mass transfer is increased by over 75%. As the frequency of the sloshing increases, as does the heat and mass transfer, rising to an increase of over 500% at a sloshing period of T=2.50 seconds.

4.2 Energy Balance

In order to ensure that the perception of the system was correct, the energy balance for a sloshing process needed to prove correct, i.e. that the amount of energy in the system is constant both before and after sloshing. Through calculation, it was aimed to find that the energy put into the system through to build pressure, was equal to the heat transferred to the liquid after sloshing. By calculating the change in internal energy, one can find how this energy flow will distribute during both a heating process and a sloshing process.

$$\Delta U = \Delta Q - \Delta W \tag{4.4}$$

$$\Delta U = \dot{Q} * \Delta t \tag{4.5}$$

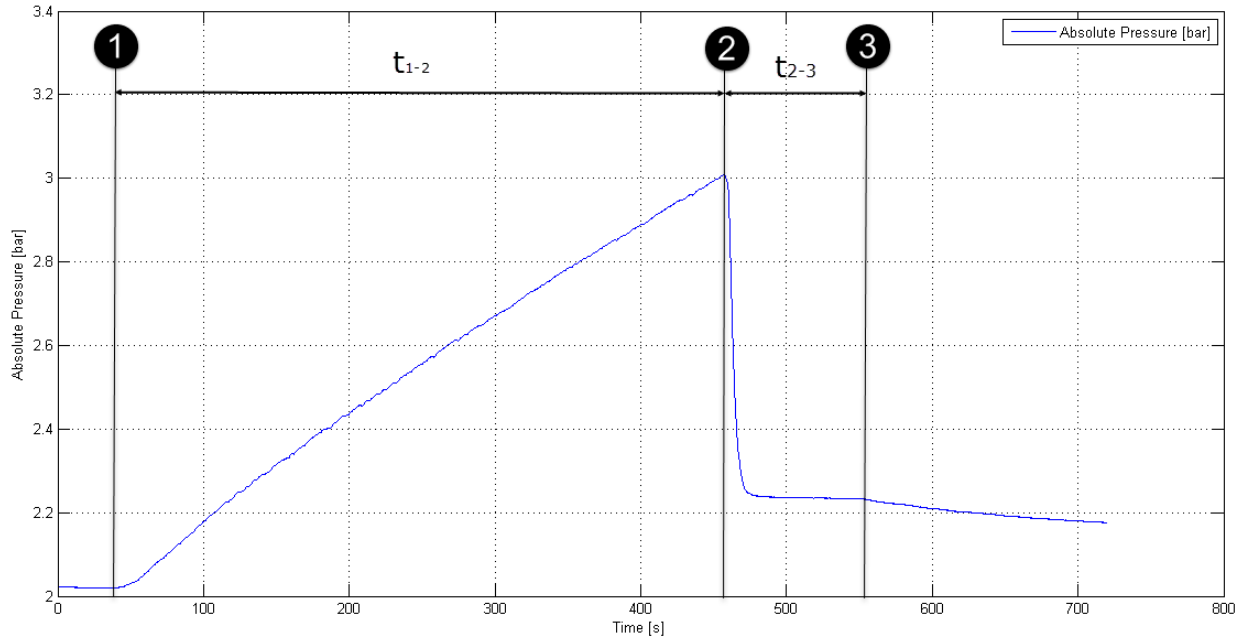

Figure 4.2: Pressure plot heating and sloshing

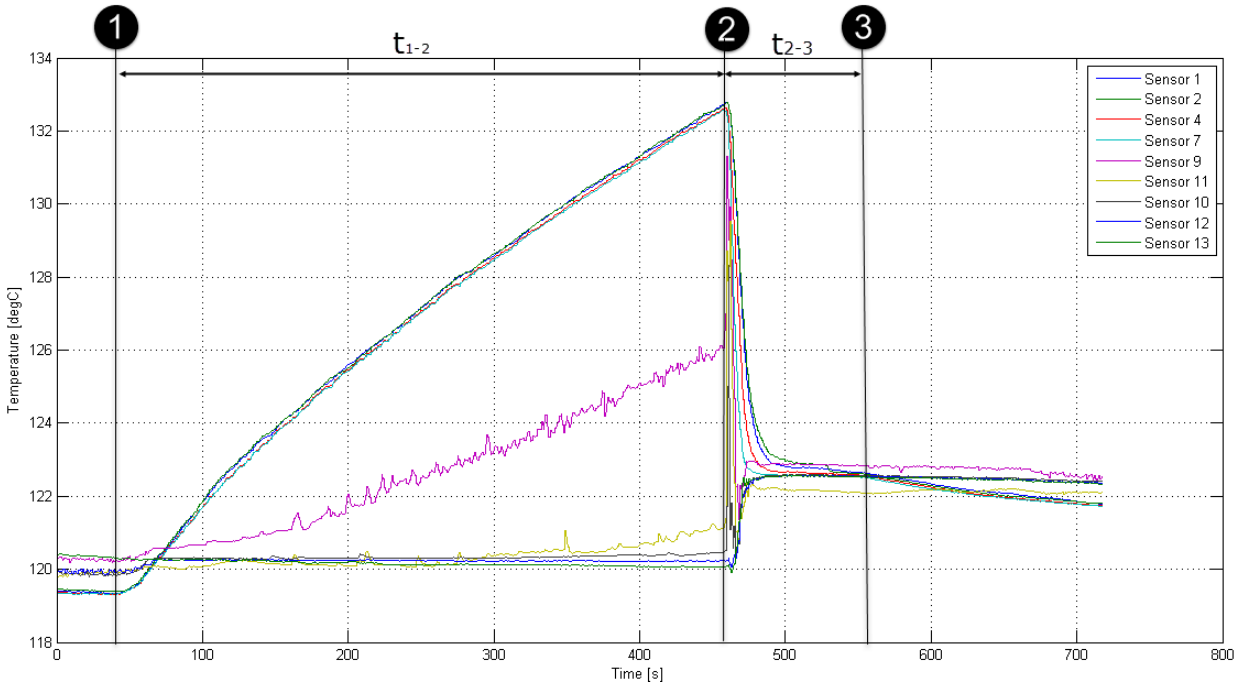

Figure 4.3: Temperature plot heating and sloshing

The first law of thermodynamics expresses the energy balance as the change in internal energy in a system during a time interval, which equals to the amount of energy transferred into the system, minus the energy transferred out of the system, as shown in equation 4.4. Equation

4.5 calculates the energy added to the system over time prior to the sloshing, as shown in figures 4.2 and 4.3. The temperature and pressure increase from t1 to t2 should correspond with the effect added from the heating element, and the subsequent pressure drop should correspond with the increase in temperature within the liquid. The parameters for the calculations are shown in table 4.3.

Table 4.3: Energy balance calculation parameters

Point	Time (in plot) [s]	$p_{abs}[bar]$	$T_{gas}[K]$	$T_{liquid}[K]$	$f_{slosh}[1/s]$	$Effect_{heater}[W]$
1	0 (39)	2.02	392.49	393.11	N/A	1460
2	418 (457)	3.01	405.88	393.38	0.53	0
3	512 (551)	2.23	395.79	395.69	N/A	0

From data in table 4.3 one can calculate how much energy is put into the system. Assuming that the heater has an efficiency of 90%, one can find through equation 4.5 that:

$$\Delta U_{heat} = 0.9 * 1460 J/s * 418 s = 549.25 * 10^3 J$$

This amount of energy has resulted in a pressure and temperature increase of:

$$\Delta p = p_2 - p_1 = 0.99 bar$$

$$\Delta T_{gas} = T_{gas2} - T_{gas1} = 13.39 K$$

$$\Delta T_{liquid} = T_{liquid2} - T_{liquid1} = 0.27 K$$

The change in liquid temperature is small, which can be blamed on oscillation in the system and errors from the thermocouples, but it is likely that some of the increase in temperature is due to condensing vapour. To find if the energy balance matches up, the change in internal energy within the tank needs to be calculated.

Neglecting the presence of air, the mass of vapour can be calculated from the ideal gas law, as shown in equation 4.1:

$$pV = mRT$$

$$m = \frac{pV}{RT}$$

Thus, it is possible to calculate the mass of vapour from equation 4.1:

$$m_1 = \frac{p_1 V}{RT_1} = \frac{2.02 * 10^5 Pa * 0.07 m^3}{461.5 \frac{J}{kgK} * 393.49 K}$$

$$m_2 = \frac{p_2 V}{RT_2} = \frac{3.01 * 10^5 Pa * 0.07 m^3}{461.5 \frac{J}{kgK} * 405.88 K}$$

$$\Delta m_{2-1} = m_2 - m_1 = 0.112 kg - 0.078 kg = 0.034 kg$$

Mass of vapour from heater during heating process:

$$\Delta m_{heater} = \dot{m}_{heater} * \Delta t = 4.91 * 10^{-4} kg/s * 418 s = 0.205 kg$$

Mass of condensed vapour during heating process is thus:

$$\Delta m_{cond} = \Delta m_{heater} - \Delta m_{2-1} = 0.205 kg - 0.034 kg = 0.171 kg$$

Increase in internal energy in gas:

$$\Delta U_G = \Delta m_{2-1} * u_g = 0.034 kg * 2529.3 * 10^3 \frac{J}{kg}$$

$$\Delta U_G = 86.36 * 10^3 J$$

Finding specific internal energy:

$$u_{fg} = u_g - u_f = 2529.3 - 546.02 = 1983.28 * 10^3 \frac{J}{kg}$$

Increase in internal energy in liquid:

$$\Delta U_L \approx \Delta m_{cond} * u_{fg}$$

$$\Delta U_L \approx 339.61 * 10^3 J$$

Total increase in internal energy in the tank:

$$\Delta U_{tot} = \Delta U_L + \Delta U_G = 425.58 * 10^3 J$$

Loss of energy to environment:

$$\dot{Q}_{loss} = U * A * (T_{tank} - T_{surroundings}) = 73 J/s$$

$$Q_{loss} = \dot{Q}_{loss} * t = 30.53 * 10^3 J$$

Energy accounted for is then:

$$\Delta U_{known} = U_{tot} + Q_{loss} = 456.14 * 10^3 J$$

Which makes the amount of energy unaccounted for:

$$\Delta U_{unknown} = \Delta U_{heat} - \Delta U_{known} = 93.11 * 10^3 J$$

Failing to account for the remainder of the energy can be down to a number of factors, with the most likely factor being the amount of condensed vapour, which represents a significant contribution to the change in internal energy.

4.3 Effect of Heat Compensation on Pressure Drop

As results in table 3.6 show, leaving the heating element on during the experiments made a small difference, where some frequencies are not subject to continuous pressure drop, although the pressure drops slightly at first. This section will investigate the matter briefly. Presented below are a selection of sloshing frequencies tested both with and without the heater initiated, and will thus provide a clearer picture of the heater's significance.

As can be seen from figure 4.4, the effect of having the heater initiated is clear. These 3 cases are where one can see that compensation is possible during low frequency sloshing, where the test with a period of T=3.50 seconds proved very stable with the electrical power used in this test. As can be seen from table 3.2, the mass flow of the heater is $4.91 \times 10^{-4} kg/s$, while the mass trans-

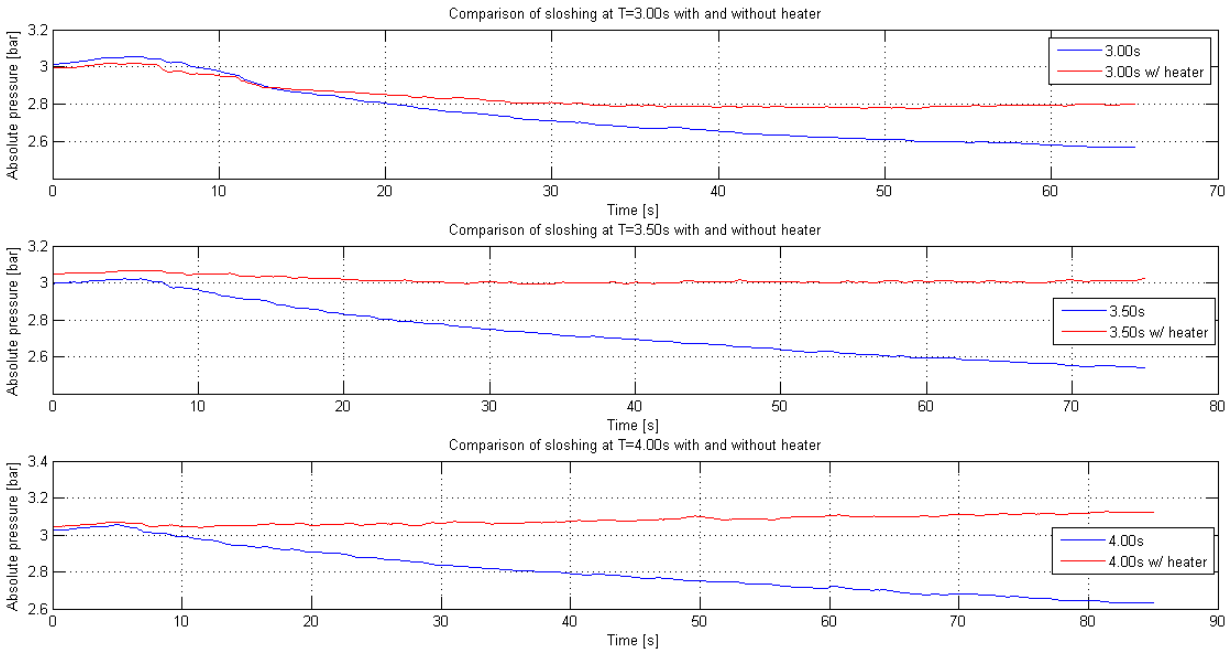

Figure 4.4: Pressure comparison with and without heater initiated during sloshing at T=3.00s, T=3.50s and T=4.00s

fer rate without heat compensation at a sloshing period of T=3.50 seconds is $2.68 \times 10^{-4} kg/s$ per table 4.2. Further, one has to take condensation into account, as some of the vapour generated will likely condensate, resulting in a higher mass transfer rate than what would be the case without heat compensation. Results in tables 3.4 and 3.6 support this idea, as the change in liquid temperature is mostly higher in the cases where heat compensation is activated, suggesting that a higher amount of mass transfer is taking place.

4.4 Pressure Drop Rate at 50% Filling Level

An observation made during testing in section 3.1 and 3.2, was that the drop rate was very cyclical, dropping significantly every time the tank's sloshing motions turned, or twice every period. This called for a closer investigation. It was first observed during the high frequency sloshing experiments, e.g. case 1-3 in figure 3.3, where one can clearly see the profile of the pressure drop. In order to see this properly, plots of the pressure drop per second was needed. At 50% filling level, a high frequency of sloshing may result in a jet, i.e. a stream of water forming, which is suspected to cause rapid condensation and pressure drop. An example of this is shown in

figure 4.5, where a stream of water is blasted forward, rapidly cooling the vapour, thus causing condensation. This fluid motion is thought to be the cause of the rapid condensation during the high frequency tests, as well as why the pressure drops significantly every half period of sloshing.

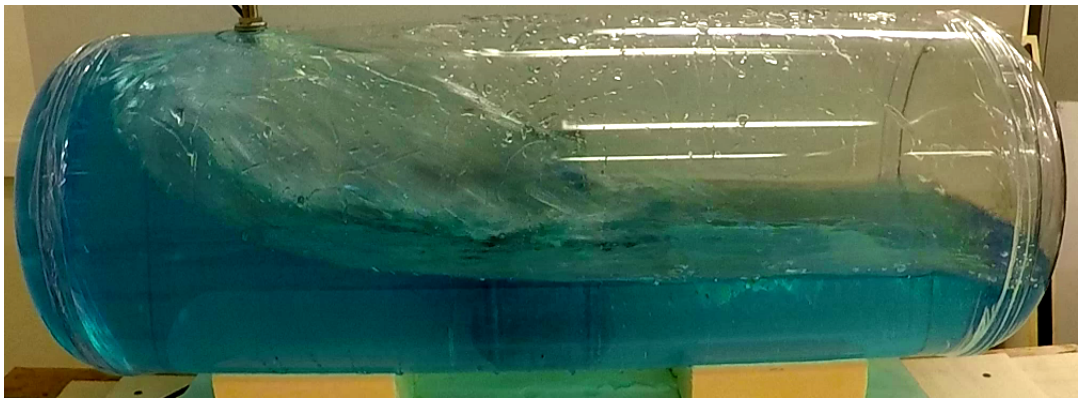

Figure 4.5: Jet forming during high frequency sloshing (Grotle et al. (2016))

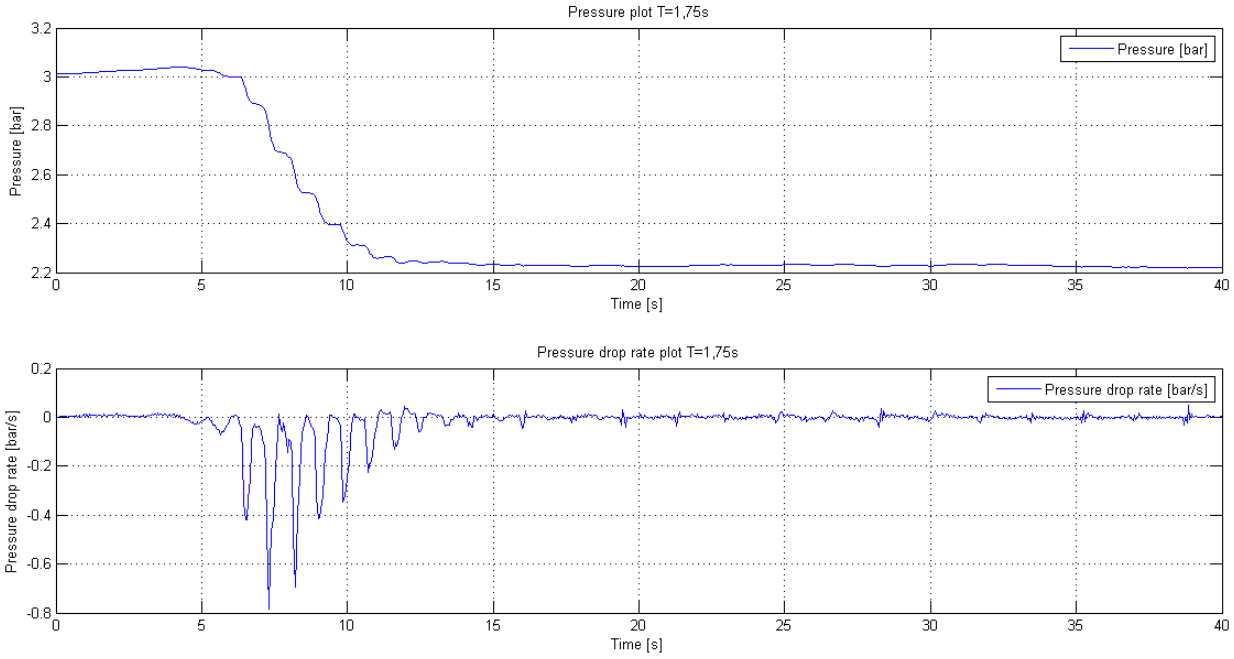

Figure 4.6: Pressure and pressure drop rate comparison at a sloshing period T = 1,75 s at 50% filling level

Figures 4.6, 4.7 and 4.8 shows clearly the cyclical nature of the pressure drop during this sloshing regime, while also supporting observations made in other sloshing experiments that it takes a few oscillation periods for the wave amplitude to break up (Ludwig et al. (2013)). When

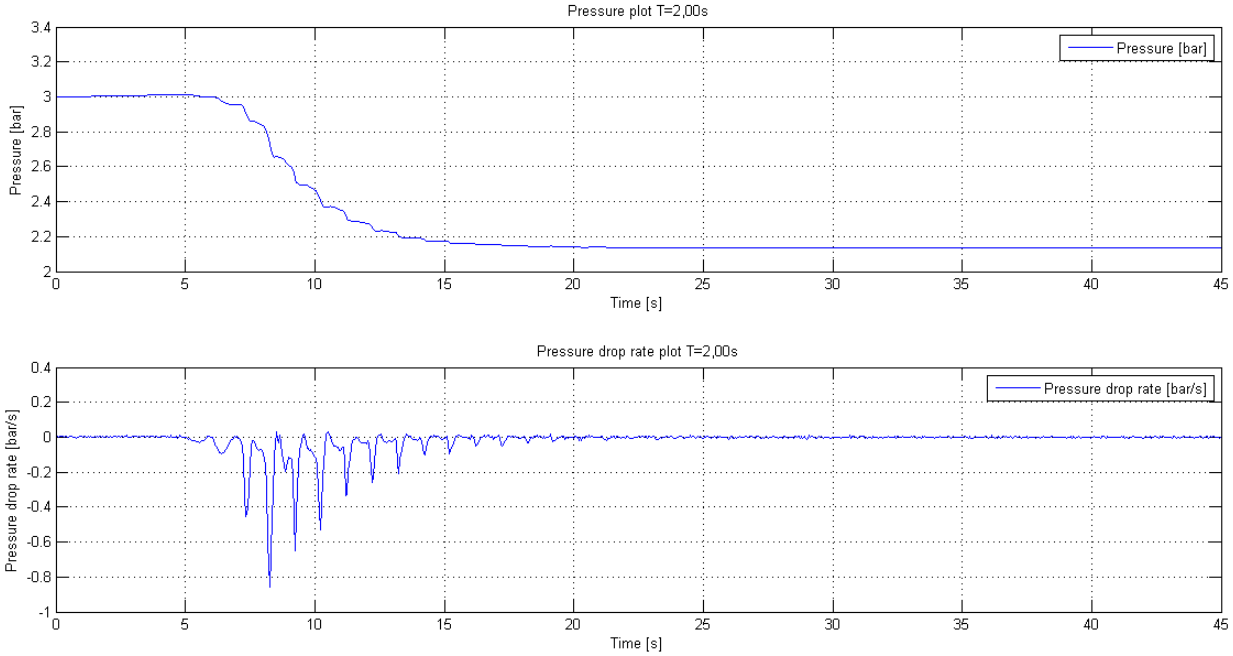

Figure 4.7: Pressure and pressure drop rate comparison at a sloshing period T = 2,00 s at 50% filling level

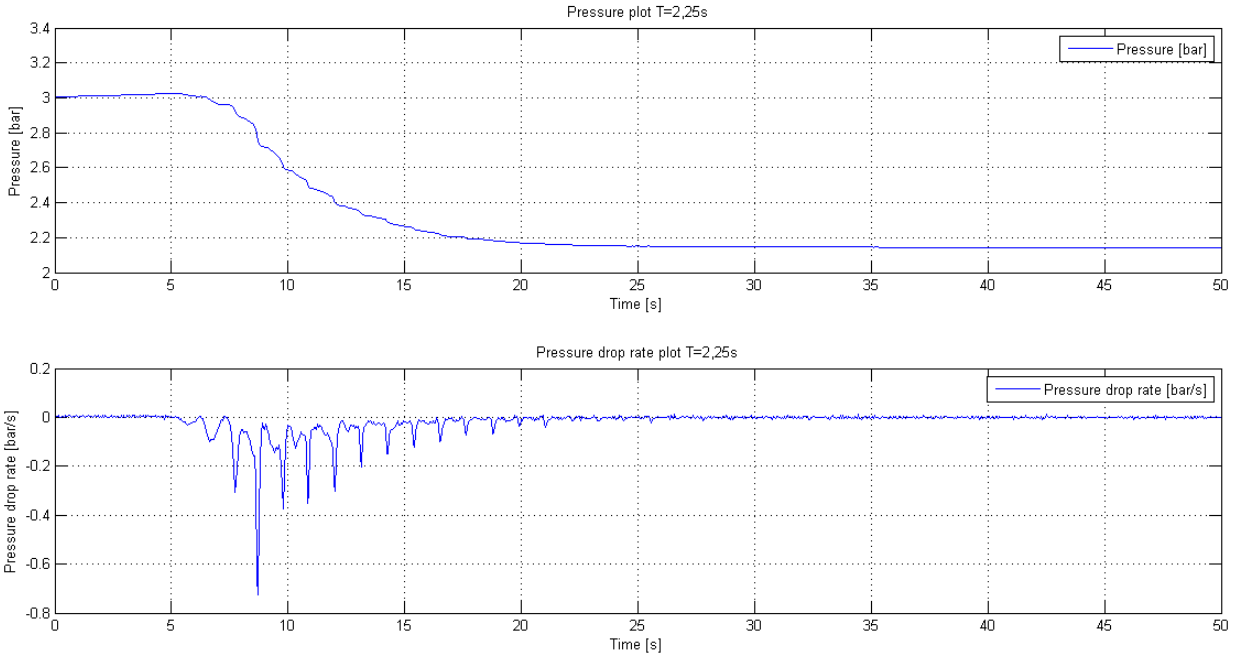

Figure 4.8: Pressure and pressure drop rate comparison at a sloshing period T = 2,25 s at 50% filling level

comparing it with the time-axis one can see that the peaks of the pressure drops correspond perfectly with every half period. This behaviour was very specific for these frequencies, where the pressure dropped much more rapidly than with the other cases; this can likely be traced back to the fluid motion inside, where the wave breaks violently at the higher frequencies, and thus causes rapid condensation and rupture of the liquid-vapour interface. To further strengthen this hypothesis, the pressure drop plots of some of the lower frequencies needs to be investigated.

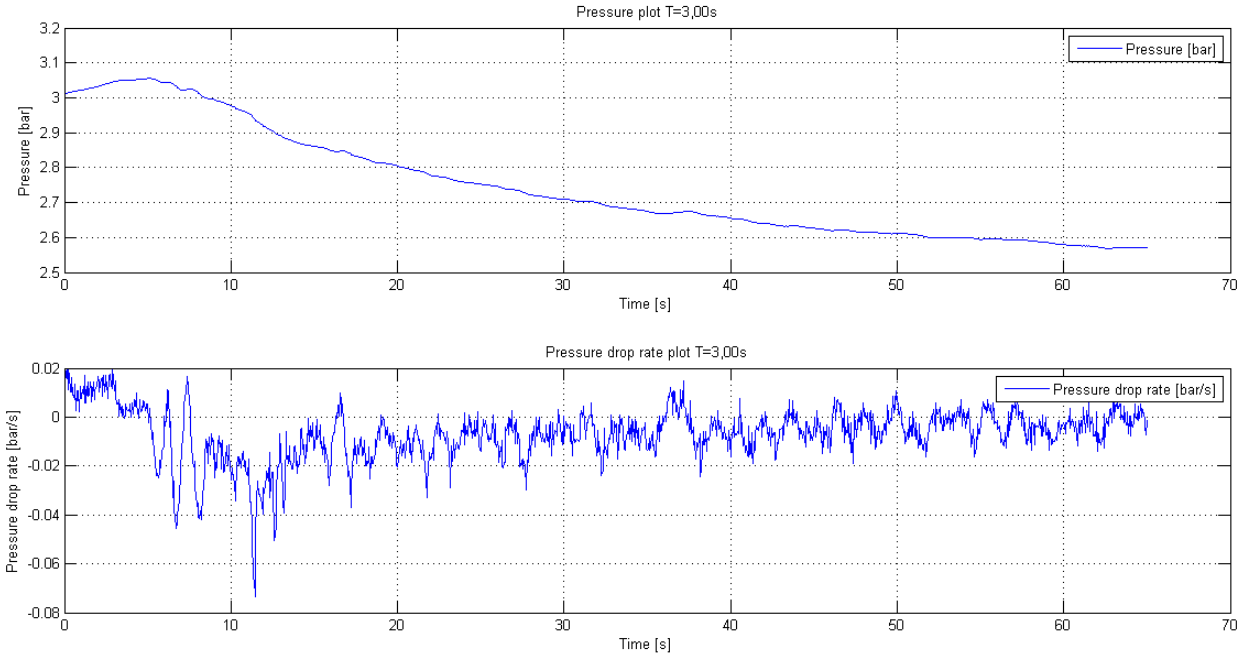

Figure 4.9: Pressure and pressure drop rate comparison at a sloshing period T = 3,00 s at 50% filling level

The behaviour of the sloshing regime in figures 4.9, 4.10 and 4.11 is very different from those shown in figures 4.6, 4.7 and 4.8. Here, the interface is most likely not breaking up in the same extent as in the tests run with high frequency. The interface seems to be oscillating, causing a more even, albeit still very cyclical pressure drop at a very small magnitude.

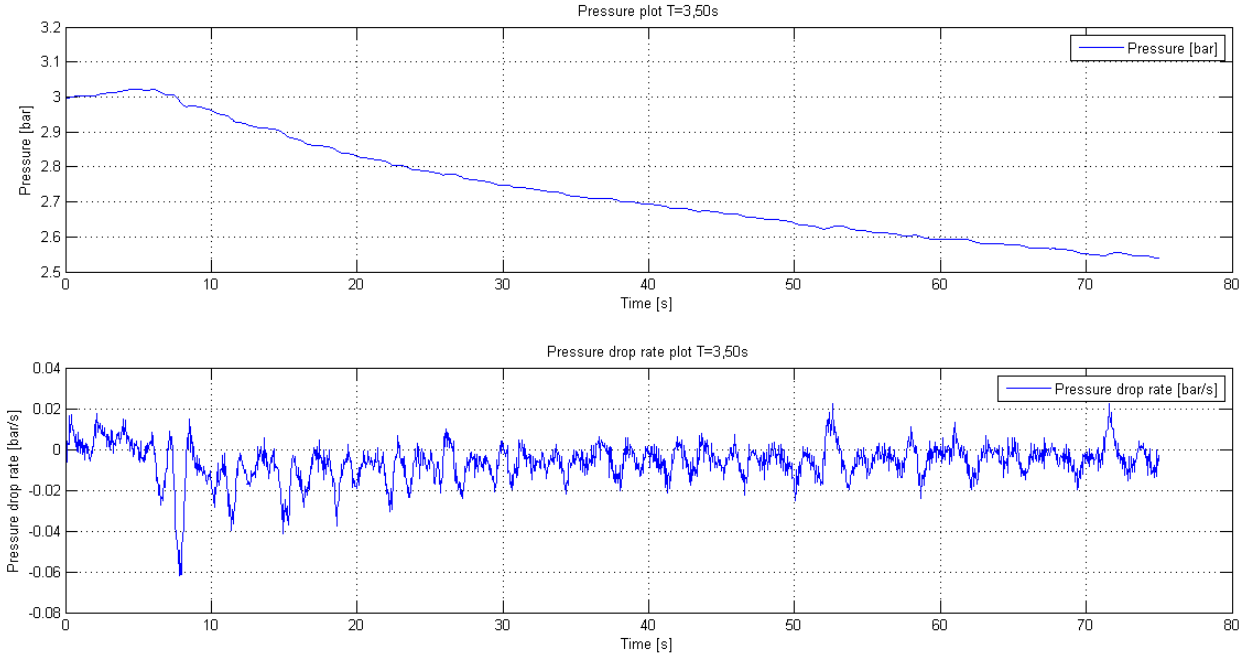

Figure 4.10: Pressure and pressure drop rate comparison at a sloshing period T = 3,50 s at 50% filling level

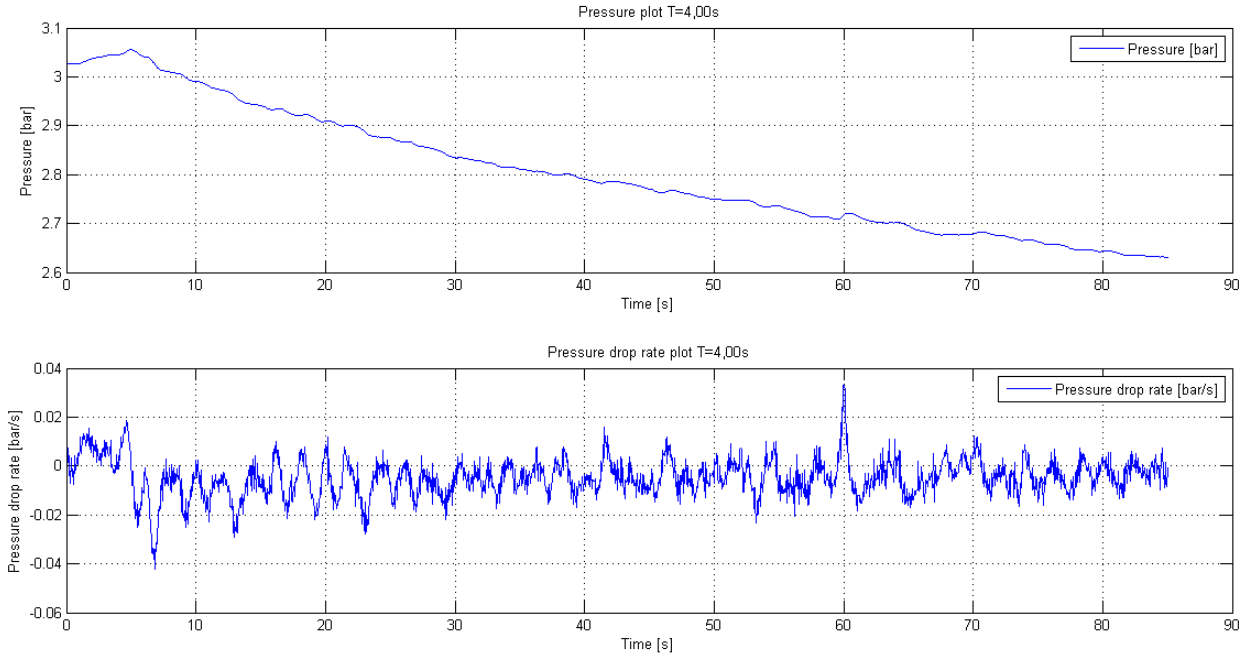

Figure 4.11: Pressure and pressure drop rate comparison at a sloshing period T = 4,00 s at 50% filling level

Chapter 5

Summary and Recommendations for Further Work

5.1 Summary and Conclusions

The main aim of the thesis work has been to identify how sloshing will affect temperature and pressure, i.e. the thermodynamical properties within an LNG fuel tank. It was seen early during the experiments that sloshing had a significant impact on both pressure and temperature within the tank, an impact that grew in magnitude with a higher frequency of sloshing. Experiments conducted with the heating element initiated showed that heat and pressure compensation of sloshing was possible at lower frequencies, whereas the more severe sloshing regime at high frequencies seems close to impossible to compensate for due to the rapid pressure drop, which has been found to be as high as 0.86 bar/s. Still, having the heater initiated reduces pressure drop to a certain extent for those cases as well.

In order to be able to perform calculations on the system, several properties had to be identified, such as the capacity and efficiency of the heater, as well as the system's heat loss to the surroundings. Finding the capacity of the heater was done through a simple experiment, which should have provided results accurate enough for the calculations to be sufficiently correct. These measurements were done with an open system, i.e. there were no counter-pressure against the vapour flow, as would be the case in a closed system, but said pressure would also act on the liquid, providing equilibrium. The heater's efficiency was found to be ranging between

83.8-95.2%, at an electrical power range between 570-2019 W. This efficiency could likely have been increased if the element was fully submerged, but with the current design this led to boiling water splashing out instead of pure vapour, which would have brought inaccurate results. The relation between power and flow is close to linear, meaning that it is possible to interpolate an approximate value for the flow at a given power setting.

A model for the heat loss of the system has been created, by calculating the heat transfer coefficient between the interior of the tank and its surroundings, found to be $U = 0.31 \frac{W}{m^2 K}$. The heat transfer coefficient has been calculated as free convection, simplifying the structure by using only the area of the tank itself, neglecting the layer of insulation outside. The result could have been compared to calculation from a conductive perspective, but has been deemed unnecessary.

Another aim of this thesis work has been to identify the heat and mass transfer between the liquid-vapour interface during sloshing. From the data registered during the sloshing experiments it was possible to calculate the rate of both heat and mass transfer, where it is found that sloshing increases both heat and mass transfer significantly. As calculations was performed for a case where no tank excitation was initiated, it was possible to see the impact sloshing had. While normal condensation had a mass transfer rate of $1.09 \times 10^{-4} kg/s$, as well as a heat transfer rate of $225.08 J/s$. For the sloshing experiment conducted at the lowest frequency at a period of T=4.00 seconds, the mass transfer rate was $1.91 \times 10^{-4} kg/s$, a 75% increase. The rate continued to increase, with the results for a sloshing period of T=2.50 seconds showing a 500% increase, as mass transfer rate was calculated to be $6.73 \times 10^{-4} kg/s$, as well as heat transfer rate of $1388.11 J/s$.

The pressure drop rate has been found to be increasing significantly as the sloshing frequency is increased, suggesting that the sloshing motion has a considerable impact on the condensation rate of the vapour. As investigated in Sec. 4.4, the pressure drop rate at sloshing periods T=1.75 s, T=2.00 s and T=2.25 s is periodical, indicating that this frequency range is where the most severe sloshing happens, as the pressure drop rate ranges from 0.72-0.86 bar/s. This in contrary to the slower frequencies, e.g. sloshing periods T=3.00-4.00 s where the pressure drop rate ranges from 0.04-0.07 bar/s.

5.2 Discussion

Maintaining full control over the system has been hard; all experiments should be conducted with close-to-identical initial conditions, but this has proven hard to control completely, as a number of actions has to be completed as the experiment starts. Pressure and temperature must be logged at exactly the same time, in order for the data to match, in addition to the motor running the sloshing having to be initiated and the heating element having to be switched off, providing a small window to complete said actions.

Conducting the experiments has also proved to be a time consuming task. Initial testing showed that temperature difference between liquid and vapour needs to be small, as the pressure drop proved too big with a large difference in temperature, this due to a large amount of energy going from vapour to the liquid through rapid condensation. A smaller difference also provides more realistic grounds for the experiment, compared to what is normal for an LNG system. This meant that the water had to be heated by running the system, i.e. vaporizing the water, for then to run the sloshing to heat the water - a process that took several hours to complete, heating the water from approximately 290 K to the predetermined 393 K, 12-13 K below saturated temperature of water at 3 bar absolute pressure, according to pressure tables found in Moran and Shapiro (2006). It is almost a certainty that there is some presence of air inside the tank, which could have led to a small difference in temperature of the vapour compared to what the saturated temperature would indicate.

Inaccuracies found during calculation of both energy balance and magnitude of heat transfer could be down to mistakes in calculations and/or assumptions of which factors affect the system. Engineering is an art of simplifying a problem sufficiently, but it may have been simplified too much in these cases, perhaps neglecting important contributors to the overall result.

5.3 Recommendations for Further Work

5.3.1 Short-term

Replicate results of interest, particularly case 1-3 as shown in tables 3.3 and 3.4 as well as in figure 3.3. It was unexpected to see that sloshing at a period of T=1.75 seconds resulted in a smaller

pressure drop than both case 2 and 3, at a sloshing period of T=2.00 seconds and T=2.25 seconds, respectively. The tests all have close-to-identical initial conditions, but as seen retrospectively, they were conducted in two different days. Thus, there may be a higher amount of air present in some of the tests when compared to the others. Still, the same can be seen happening during the same tests conducted with the heater on, as shown in figure 3.10. Nonetheless, some of the results should be attempted replicated by conducting a new series of experiments, in order to verify the results.

5.3.2 Medium-term

Implement control regulation in order to maintain pressure, in addition to installing sensors for measuring and logging electrical power used as well as a flow sensor to monitor the capacity of the electrical heater properly. Calculating the heat and mass transfer rate from results found in Sec. 3.4. in this thesis could help solve this problem further, calculating the condensation rate in the system while heat compensation is activated.

5.3.3 Long-term

Perform computational fluid dynamics (CFD) analysis of the sloshing regime investigated, or build transparent model of sloshing tank, in order to link results to sloshing motion inside of tank. This could further aid the understanding of the results.

Bibliography

Arndt, T. (2011). *Sloshing of Cryogenic Liquids in a Cylindrical Tank under normal Gravity Conditions*. Universtität Bremen.

Das, S. and Hopfinger, E. (2009). Mass transfer enhancement by gravity waves at a liquid–vapour interface. *International Journal of Heat and Mass Transfer*, 52(5):1400–1411.

Grotle, E. L., Bihs, H., Pedersen, E., and Æsøy, V. (2016). CFD simulations of non-linear sloshing in a rotating rectangular tank using the level set method. In *ASME 2017 36th International Conference on Ocean, Offshore and Arctic Engineering*, pages V002T08A019–V002T08A019. American Society of Mechanical Engineers.

HBM (2017). P8AP. https://www.hbm.com/en/2484/p8ap-for-static-and-\dynamic-liquid-and-gas-pressures/. Accessed: 2017-04-07.

Ludwig, C., Dreyer, M., and Hopfinger, E. (2013). Pressure variations in a cryogenic liquid storage tank subjected to periodic excitations. *International Journal of Heat and Mass Transfer*, 66:223–234.

Moran, J. and Shapiro, N. (2006). *Fundamentals of Engineering Thermodynamics*. Wiley, Chichester, England, 5th edition.

Omega (2017). Thermocouples. http://www.omega.com/prodinfo/thermocouples.html. Accessed: 2017-04-07.

Appendix A

Article Draft

The Effect of Sloshing on a Tank Pressure Build-Up Unit

Håvard Bolstad Banne
Norwegian University of Science and Technology

Abstract: This paper investigates the effect of sloshing on a tank pressure build-up unit (PBU), where the temperature and pressure change from sloshing has been investigated experimentally. Several of the properties of the system are identified, such as the efficiency of the heater, found to be ranging between 83.8-95.2% depending on the power used, as well as the heat transfer coefficient between the tank and its surroundings, calculated to be $U = 0.31 W/m^2K$. Sloshing experiments are conducted at 50% filling level, both with and without the heater initiated. The sloshing periods ranges from T=1.75s to T=4.00s, where the general results show that sloshing have a significant effect on heat and mass transfer in the system, while also showing that high frequency of sloshing accelerates the heat and mass transfer process further. Having the heater initiated has proven to reduce change in pressure, and can thus be tuned to compensate pressure drop at lower frequencies. The rate of heat and mass transfer is calculated as well, showing clearly the impact of sloshing.

Keywords: Sloshing; experiments; heat transfer; mass transfer

Introduction

Utilizing liquefied natural gas (LNG) as a fuel for ship transportation has shown great promise, due to its availability, cost effectiveness and environmental friendliness compared to traditional MDO. One of the issues of using LNG is the amount of space it requires in its gas state; thus, keeping it in a liquid state is a must. Implementing a pressure build-up unit (PBU) is a way of solving this, as the PBU keep the tank pressurized, in addition to pushing the LNG through a vaporizer and into the engine, as shown in figure 1.

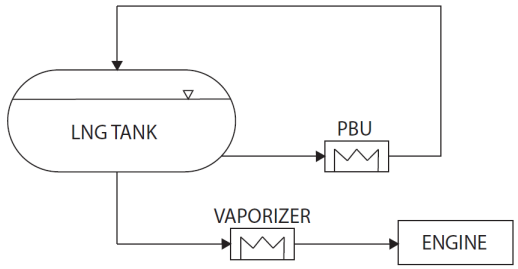

Figure 1. LNG fuel system with a PBU

The sloshing regime, or tank excited heat and mass transfer has been investigated for years, particularly in relation to fuel tanks in space rockets (Arndt, 2011), in addition to design of roads and dams, but the topic is still relatively new within the maritime sector in relation to LNG. Sloshing is generally a mostly unwanted behaviour of dynamic fluid, and has the potential to result in pressure drop within the tank, with engine shutdown as a possible consequence. The sloshing regime will thus be investigated, finding how the severity of the sloshing affect the system.

Setup of Experimental Rig

An insulated tank has been designed and built in the laboratory at NTNU Aalesund, where several temperature sensors and a pressure sensor has been installed. This tank has been expanded to include piping in and out of a heating element, contained within a small steel container. Figure 2 shows the main arrangements of the rig.

Table 1
Experiment instrumentation.

Device	Type	Range
Temp.sensor	Type T	-250-350 [°C]
Pressure sensor	HBM P8AP	0-20 [bar]
Heating element	Høiax	0-3000 [W]
Power supply	Philips	0-260 [V]
El.motor	MAC800-D2	750 [W] @ 3000 rpm

Limitations

In order to simplify the experiments, water has been used as testing medium, due to it being both easily available and significantly easier to handle than LNG, which would have required a complicated testing procedure in order to keep it sufficiently cooled and pressurized. Water does have completely different physical properties compared to LNG, but these experiments are primarily conducted to observe the physical process.

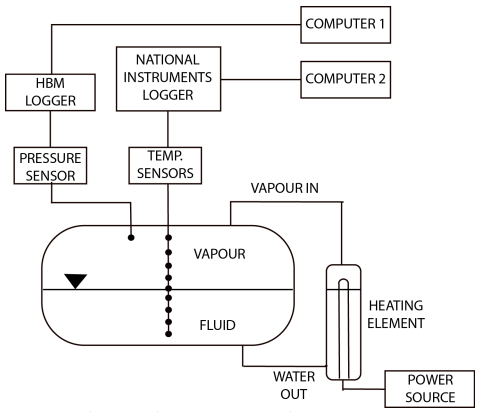

Figure 2. Experiment instrumentation arrangement

For the calculations, it has been assumed that there is no presence of air inside the tank, only saturated vapour. As it is hard to control the amount of air inside, it was decided to disregard the presence of air completely. An average temperature of both vapour and liquid has often had to be assumed, due to the variation of temperature in the different layers of vapour and liquid.

Experiment Procedure

Before the experiments can be conducted, the test medium in the tank is heated from approximately 15C to 120C. To increase the temperature in the system as efficiently as possible, sloshing is regularly utilized to transfer the heat energy from vapour to liquid.

System Heat Loss

The heat loss of the system was mapped by heating up the contents of the tank, for then to switch off the heating element, letting it cool down, the vapour condensing as the liquid vapour interface is at rest. When temperatures of gas and liquid are equal, the proceeding loss is what goes out to its environment.

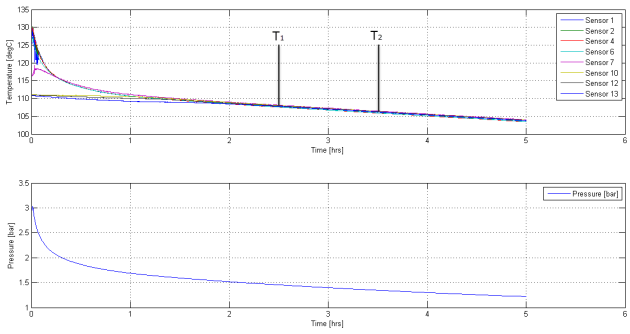

Figure 3. Tank cooling over a 5 hour period

As one can see in figure 3, the temperature of gas and liquid are close to equal after approximately 2 hours; the proceeding drop in temperature in the system is due to heat loss to the surroundings. The rate of energy transfer to the surroundings can be expressed through:

$$\dot{Q}_{loss} = U * A_{tank} * (T_{tank} - T_{surroundings}) \tag{1}$$

$$\dot{Q}_{cooling} = \sum m * C_v * \frac{dT}{dt} \tag{2}$$

By use of equations 1 and 2, one can solve for the heat transfer coefficient, which gives:

$$U = \frac{\sum m * C_v * \frac{dT}{dt}}{A * (T_{tank} - T_{surroundings})} \tag{3}$$

Which gives us:

$$U = 0.31 \frac{W}{m^2 K}$$

Heater Efficiency

Finding the amount of water the system was able to evaporate was important, therefore the mass flow was measured at different effects. By keeping a bucket filled with water at the same level as it would have been at 50 % filling level within the tank, it was possible for find the amount of water being evaporated by measuring the remaining mass of water in the bucket with a scale every minute for a period of at least 10 minutes. Thus, it was also possible to find the approximate efficiency of the heater. The electrical power was measured with a voltmeter coming out from the power source. Setup of the experiment is shown in figure 4 below.

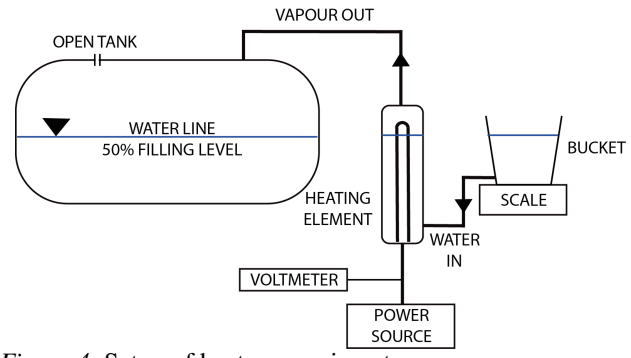

Figure 4. Setup of heater experiment

From the results found in this experiment, as shown in table 2, it is possible to find the effect necessary to vaporize the measured flow, utilizing the latent heat of evaporation for water, assumed to be Δhfg=2 257 000 J/kg for this case.

$$\dot{Q}_{latent} = \Delta hfg * \dot{m} \tag{4}$$

Table 2
Heater efficiency.

P_{el} [W]	$\dot{m}$ [kg/s]	$\dot{Q}_{vap}$ [W]	$\dot{Q}_{heat}$ [W]	$\dot{Q}_{loss}$ [W]	η [%]
570	$1{,}83\times10^{-4}$	413	64,6	92,4	83,8
982	$3{,}37\times10^{-4}$	761	119,9	101,1	89,7
1461	$4{,}91\times10^{-4}$	1105	172,9	183,1	87,5
2019	$7{,}37\times10^{-4}$	1663	260,0	96,0	95,2

$$\dot{Q}_{heat} = \dot{m} * C_p * \Delta T \tag{5}$$

$$\eta = \left(\frac{\dot{Q}_{total}}{Power_{electrical}}\right) \tag{6}$$

Where:

$$\dot{Q}_{total} = \dot{Q}_{vaporize} + \dot{Q}_{heat} - \dot{Q}_{loss}$$

From equation 4 one can calculate the power necessary to evaporate the measured flow. The data was measured once a steady state had been achieved, which should exclude the effect required to heat the entire contents of the tank, leaving only the water coming in to the container, which needs to be heated from approximately 15°C to 100°C. From equation 5 one finds the effect needed to heat a certain flow of water by utilizing the specific heat capacity of the water at constant pressure, which as an open system, this is assumed to be. Equation 6 calculates the efficiency of the heater.

Sloshing at 50% Filling Level

Through sloshing at different frequencies one can observe how the severity of the sloshing affects the pressure drop as well as the mixing of the temperature. These experiments were conducted in order to observe how severe wave motion can affect an LNG fuel tank. In tables 3 and 4 one can see the initial conditions and results from the experiment, respectively. Sloshing was run for 20 periods at different frequencies, thus representing a clearer picture of how the different conditions would affect the system. In addition, a reference case was included where no tank excitation was initiated. For these tests, the heating element was switched off during the experiments to make sure no additional energy were added to the system.

As can be seen in figure 5, the frequency of the sloshing have a huge significance on the energy transfer. Even low sloshing frequency, such as in case 4-6, shows clear difference compared to the case where no tank excitation is initiated.

Table 3
Initial conditions sloshing at 50% filling level.

Case –	T_G [K]	T_L [K]	ΔT_0 [K]	$\lvert p_0 \rvert$ [bar]
1	405.95	393.46	12.49	3.04
2	405.88	393.09	12.79	3.00
3	405.31	393.08	12.23	3.01
4	406.05	393.59	12.46	3.06
5	405.80	393.05	12.75	3.02
6	406.16	393.35	12.81	3.06
7	405.80	393.08	12.72	3.02

Table 4
Results sloshing at 50% filling level.

Case –	T [s]	ΔT_G [K]	ΔT_L [K]	Δp [bar]	$\lvert dp/dt \rvert_{max}$ [bar/s]
1	1.75	-10.57	1.87	-0.82	0.78
2	2.00	-11.51	1.23	-0.87	0.86
3	2.50	-10.87	0.87	-0.84	0.47
4	3.00	-5.67	0.09	-0.49	0.07
5	3.50	-5.59	-0.01	-0.48	0.06
6	4.00	-4.77	-0.07	-0.43	0.04
7	N/A	-2.95	-0.03	-0.25	0.02

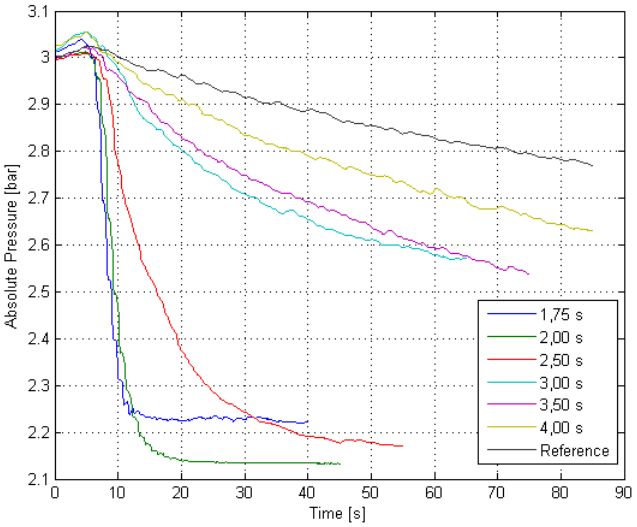

Figure 5. Pressure plot of case 1-7 at 50% filling level

Sloshing at 50% Filling Level - Heat Compensation

A set of experiments were conducted in order to see the significance of keeping the heating element on during the tests, as well as seeing if it was possible to compensate the pressure drop.

One can clearly see the significance of having the heating element on during the tests, where can see especially at T=4.00 seconds, where the pressure keeps rising despite

Table 5
Initial conditions sloshing at 50% filling level with heater on.

Case –	T_G [K]	T_L [K]	ΔT_0 [K]	$\lvert p_0 \rvert$ [bar]
1	406.04	393.56	12.48	3.05
2	405.77	393.28	12.49	3.02
3	405.61	392.87	12.74	3.01
4	405.76	393.09	12.67	3.02
5	406.45	393.42	13.03	3.07
6	406.31	393.57	12.72	3.07

Table 6
Results sloshing at 50% filling level with heater on.

Case –	T [s]	ΔT_G [K]	ΔT_L [K]	Δp [bar]	$\lvert dp/dt \rvert_{max}$ [bar/s]
1	1.75	-9.76	2.48	-0.77	0.73
2	2.00	-10.84	1.32	-0.83	0.89
3	2.50	-9.59	0.67	-0.78	0.50
4	3.00	-2.61	-0.09	-0.22	0.09
5	3.50	-0.73	0.08	-0.05	0.04
6	4.00	0.63	-0.02	0.05	0.04

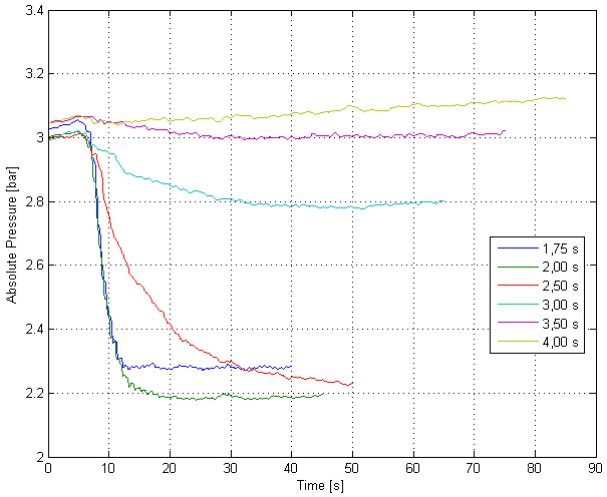

Figure 6. Pressure plot of case 1-6 at 50% filling level with heater on

tank excitation. T=3.50 seconds seems very well balanced in terms of energy added from the heating element compared to energy transferred due to sloshing. Comparing it with the previous test will illustrate the heater's significance better, as can be seen in figure 7.

Heat Transfer Over the Liquid-Vapour Interface

It has been shown from the results that sloshing increases energy transfer over the liquid-vapour interface. Here, it will be investigated the rate of heat and mass transfer produced

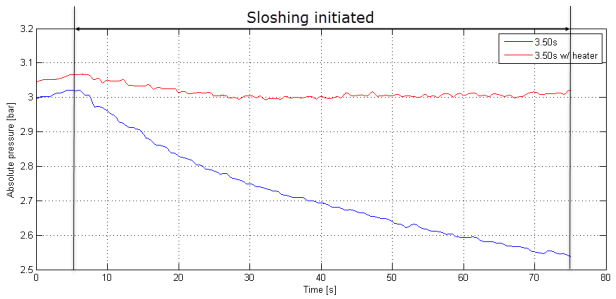

Figure 7. Comparison of sloshing with and without heater at T=3.50 seconds at 50% filling level

by sloshing. By neglecting any presence of air, calculating the mass of vapour can be done by use of the ideal gas law (equation 7) at set points during the sloshing experiments. Thus, it is possible to find the amount of vapour condensing during the experiment. A selection of results of interest will be used in these calculations, as found in tables 3 and 4.

$$pV = mRT \tag{7}$$

The rate of mass transfer can be calculated by finding the change in mass through equation 7:

$$\frac{dm_G}{dt} = \frac{m_{G2} - m_{G1}}{t_2 - t_1} \tag{8}$$

Further, the rate of energy transfer can be expressed as:

$$\frac{dU}{dt} = \frac{(m_{G2}u_{G2} - m_{G1}u_{G1}) + (m_{L2}u_{L2} - m_{L1}u_{L1})}{t_2 - t_1} \tag{9}$$

In addition to calculating the effect sloshing has on the rate of heat and mass transfer, the case with no tank excitation will be included, in order see the difference. Noted in table 7 as 'not applicable' (N/A).

Table 7
Results rate of heat and mass transfer

$T_{sloshing}[s]$	$\lvert dm_G/dt \rvert \times 10^{-4}[kg/s]$	|dU/dt| [J/s]
2.50	6.73	1388.11
3.00	3.34	689.48
3.50	2.68	553.20
4.00	1.91	396.06
N/A	1.09	225.08

As table 7 shows clearly, sloshing has a substantial impact on heat and mass transfer. Even with a slow sloshing period, e.g. T=4.00 seconds, the heat and mass transfer is increased by over 75%. As the frequency of the sloshing increases, as does the heat and mass transfer, rising to an increase of over 500% at a sloshing period of T=2.50 seconds.

Pressure Drop Rate at 50% Filling Level

An observation made during testing, was that the drop rate was very cyclical, dropping significantly every time the tank's sloshing motions turned, or twice every period. This called for a closer investigation. It was first observed during the high frequency sloshing experiments, e.g. case 1 and 2 in figure 5, where one can clearly see the profile of the pressure drop. In order to see this properly, plots of the pressure drop per second was needed.

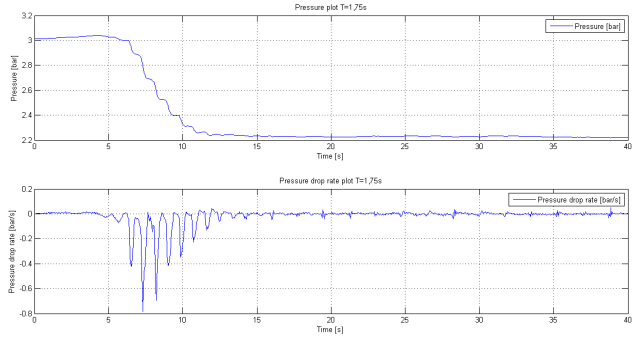

Figure 8. Pressure and pressure drop rate comparison at a sloshing period T = 1.75 s at 50% filling level

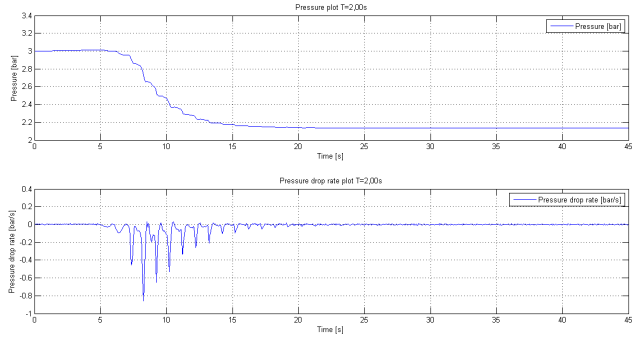

Figure 9. Pressure and pressure drop rate comparison at a sloshing period T = 2.00 s at 50% filling level

One can clearly see from figures 8 and 9 that the peaks of the pressure drop rate match with every half period, suggesting that the the fluid motion inside causes rapid condensation, thus rapid heat and mass transfer. One can also see that it takes a few oscillation periods for the wave amplitude to break up, correlating with observations made in other sloshing experiments (Ludwig et al., 2013).

In order to compare these observations, similar plots were created from cases tested at a lower frequency, where the liquid-vapour interface would not break up in the same manner. As can be seen in table 4, the maximum pressure drop rate, dp/dt, is very small compared to the tests conducted at a higher frequency, which is shown clearly in figures 10 and 11. Rather than having clear spikes in pressure drop, it is more of a oscillation in these tests, suggesting a very different sloshing regime than in figures 8 and 9.

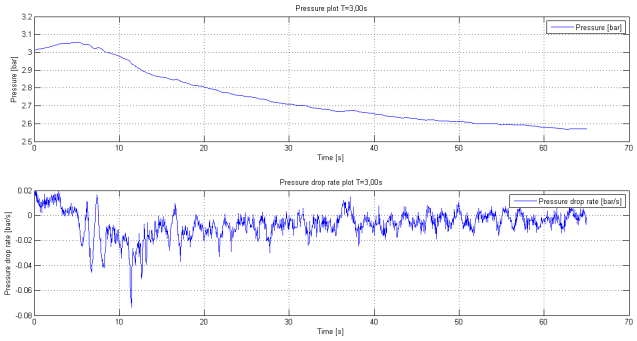

Figure 10. Pressure and pressure drop rate comparison at a sloshing period T = 3.00 s at 50% filling level

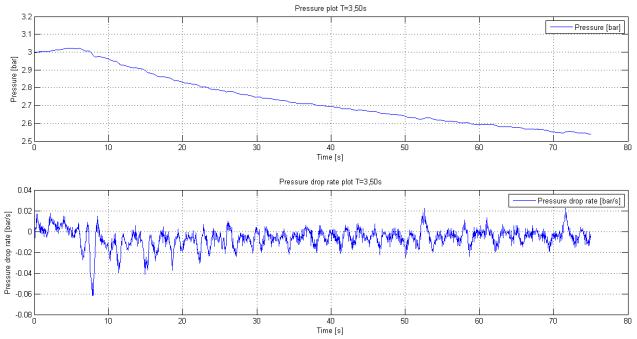

Figure 11. Pressure and pressure drop rate comparison at a sloshing period T = 3.50 s at 50% filling level

Conclusion

The main aim of the thesis work has been to identify how sloshing will affect temperature and pressure, i.e. the thermodynamical properties within an LNG fuel tank. It was seen early during the experiments that sloshing had a significant impact on both pressure and temperature within the tank, an impact that grew in magnitude with a higher frequency of sloshing. Experiments conducted with the heating element initiated showed that heat and pressure compensation of sloshing was possible at lower frequencies, whereas the more severe sloshing regime at high frequencies seems close to impossible to compensate for due to the rapid pressure drop, which has been found to be as high as 0.86 bar/s.

Finding the capacity of the heater was done through a simple experiment. The heater's efficiency was found to be ranging between 83.8-95.2%, at an electrical power range between 570-2019 W. This efficiency could likely have been increased if the element was fully submerged, but with the current design this led to boiling water splashing out instead of pure vapour, which would have brought inaccurate results.

The relation between power and flow is close to linear, meaning that it is possible to interpolate an approximate value for the flow at a given power setting.

A model for the heat loss of the system has been created, by calculating the heat transfer coefficient between the interior of the tank and its surroundings, found to be $U = 0.31 \frac{W}{m^2 K}$. The heat transfer coefficient has been calculated as free convection, simplifying the structure by using only the area of the tank itself, neglecting the layer of insulation outside.

The pressure drop rate has been found to be increasing significantly as the sloshing frequency is increased, suggesting that the sloshing motion has a considerable impact on the condensation rate of the vapour. The pressure drop rate at sloshing periods T=1.75 s, T=2.00 s and T=2.25 s is periodical, indicating that this frequency range is where the most severe sloshing happens, as the pressure drop rate ranges from 0.72-0.86 bar/s. This in contrary to the slower frequencies, e.g. T=3.00-4.00 s where the pressure drop rate ranges from 0.04-0.07 bar/s.

Another aim of this thesis work has been to identify the heat and mass transfer between the liquid-vapour interface during sloshing. From the data registered during the sloshing experiments it was possible to calculate the rate of both heat and mass transfer, where it is found that sloshing increases both heat and mass transfer significantly.

References

Arndt, T. (2011). *Sloshing of cryogenic liquids in a cylindrical tank under normal gravity conditions*. Universtität Bremen.

Ludwig, C., et al. (2013). Pressure variations in a cryogenic liquid storage tank subjected to periodic excitations. *International Journal of Heat and Mass Transfer*, *66*, 223–234.

Appendix B

Additional Information

B.1 Parameters For Experimental Rig

If one is to replicate or conduct a new set of experiments, the relation between sloshing frequency, period and motor RPM can be calculated through:

$$RPM_{motor} = 3000 * f_{sloshing}$$

$$f_{sloshing} = \frac{1}{T_{sloshing}}$$

$$T_{sloshing} = \frac{1}{f_{sloshing}}$$

In addition, most of the parameters used for testing in this thesis is shown in table B.1 below:

Table B.1: Parameters of Experimental Rig

$T_{sloshing}[s]$	$f_{sloshing}[1/s]$	$RPM_{motor}[rpm]$
1.75	0.57	1714
2.00	0.50	1500
2.25	0.44	1333
2.50	0.40	1200
2.75	0.36	1090
3.00	0.33	1000
3.25	0.31	923
3.50	0.29	857
3.75	0.27	800
4.00	0.25	750